The Medicinal Applications of Imidazolium Carbene−Metal Complexes

Khadijah M. Hindi,[†] Matthew J. Panzner,[†] Claire A. Tessier,[†] Carolyn L. Cannon,[‡] and Wiley J. Youngs*[,†]

Department of Chemistry, The University of Akron, Akron, Ohio 44325-3601, and Department of Pediatrics and Molecular Microbiology and Microbial Pathogenesis, Washington University School of Medicine, St. Louis, Missouri 63110

Received October 27, 2008

Downloaded by UNIV MAASTRICHT on August 28, 2009 | http://pubs.acs.org
Publication Date (Web): July 6, 2009 | doi: 10.1021/cr800500u

Contents

1. Introduction

Öfele and Wanzlick reported the synthesis of the first N-heterocyclic carbene (NHC)−metal complexes in 1968.[1,2] The isolation of the first free carbene by Arduengo in 1991 set the scene for an ever-growing interest and advancement in the field of N-heterocyclic carbene chemistry.[3] Shortly thereafter, the use of these ligands in organometallic chemistry, particularly in catalysis, dramatically increased.[4,5]

N-heterocyclic carbenes are neutral two-electron donors with an ability to bond to both hard and soft metals making them more versatile ligands than phosphines.[6] As an added advantage, not only are NHCs easier to synthesize and functionalize than phosphines but they also form a stronger bond to metals and therefore form more stable metal

Khadijah Hindi was born in Amman, Jordan. She received a B.S. with honors in chemistry from the University of Akron in the fall of 2003. She earned a Ph.D. degree in the summer of 2008 at the University of Akron, under the direction of Professor Wiley J. Youngs, focusing on the synthesis and study of silver N-heterocyclic carbene complexes, including their application as antitumor agents, as well as antimicrobials active against a wide array of Gram-negative and Gram-positive bacteria. Currently, she is a Postdoctoral Fellow with Dr. Carolyn Cannon at Washington University School of Medicine in St. Louis, MO.

* To whom correspondence should be addressed. Phone: (330) 972-5362. E-mail: youngs@uakron.edu.
[†] The University of Akron.
[‡] Washington University School of Medicine.

10.1021/cr800500u CCC: $71.50 © 2009 American Chemical Society
Published on Web 07/06/2009

Matthew Panzner grew up in Copley Township several miles west of Akron, Ohio. He received his B.S. in chemistry from the University of Akron in 2001. He subsequently entered graduate school and received his Ph.D. under the guidance of Wiley Youngs in 2006. During his time in the Youngs laboratory, he studied the synthesis of N-heterocyclic carbene metal complexes with an emphasis on silver. He currently works as a Project Manager for Wiley Youngs focusing on the advancement of silver carbene antimicrobials and the synthesis and study of new inorganic backbone polymer fuel cell membrane materials.

Claire Tessier began her scientific career as an ACS Project SEED student in the laboratory of Klaus Wulff at the University of Vermont. She continued her studies at the University of Vermont and received a B.S. in chemistry in 1975. In 1982, she earned a Ph.D. degree, under the direction of O. T. Beachley, Jr., from the State University of New York at Buffalo. In 1981−1982, she completed a postdoctoral position with D. F. Shriver at Northwestern University. She began her current position as a professor at the University of Akron in 1990. Her research interests include phosphorus and silicon-based inorganic-backbone polymers, biomineralization, and metal-NHC chemistries.

Carolyn Cannon is a native Texan, who graduated from Texas A&M in 1982 with a B.S. in bioengeneering. She received a M.S. in electrical engineering from Worcester Polytechnic Institute in Massachusetts in 1985 before returning to Texas to pursue a medical deqree and further graduate training. She obtained her medical degree from the University of Texas Medical School at Houston and a Ph.D. in Physiology and Cell Biology from the associated Graduate School of Biomedical Sciences, both in 1993. She was a pediatric resident at the Children's Hospital in Boston and continued training as a pediatric pulmonary fellow, until Dr. Cannon subsequently joined the faculty a Harvard Medical School in 1999. She held a joint appointment as a Research Fellow at The Channing Laboratory where she completed postdoctoral training. In 2003, Dr. Cannon joined the faculty at Washington University in St. Louis and acts as the Co-Director of the Cystic Fibrosis Center at St. Louis Children's Hospital. Dr. Cannon's laboratory has focused on the pathogenesis of infection in cystic fibrosis, as well as the development of the silver−carbene antimicrobials synthesized in Dr. Youngs' laboratory to treat these infections. Thus, the efforts in the laboratory center on the confluence of molecular microbiology, microbial pathogenesis, drug discovery, pharmocology, toxicology, and respiratory cell biology.

Wiley Youngs is originally from northern New York State. He received a B.A. in Psychology from the State University of New York at Albany and returned to school to further pursue his undergraduate education in chemistry at SUNY Potsdam and Clarkson University. He received his Ph.D. in 1980 under the supervision of Melvyn Churchill at SUNY Buffalo. Following a postdoctoral fellowship with James Ibers at Northwestern University, he joined the faculty at Case Western Reserve University in 1983. In 1990, he moved to the University of Akron where he is currently a Full Professor of Chemistry. Dr. Youngs' research interests include N-heterocyclic carbenes, silver-based antimicrobials, metal-based cancer drugs, and fuel cell membrane materials.

Downloaded by UNIV MAASTRICHT on August 28, 2009 | http://pubs.acs.org
Publication Date (Web): July 6, 2009 | doi: 10.1021/cr800500u

complexes than metal−phosphine complexes.[7,8] The N-heterocyclic carbene ligands interact with metal centers primarily through strong σ-donation and to a lesser degree through π-back-donation (Figure 1).[9,10]

Ghosh and co-workers[11−16] as well as others[17−19] took special interest in the exceptional stability of several metal−NHC complexes and conducted in depth analyses in order to gain better insights into the structure and bonding. In particular, the metal−ligand donor−acceptor interactions were inspected using charge decomposition analysis (CDA). CDA is a tool used to quantitatively estimate the degree of NHC $\rightarrow$ metal σ-donation, designated by d, and NHC $\leftarrow$ metal π-back-donation, designated by b.[20,21] Thus a higher d/b ratio emphasizes the ability of NHC to function as an effective σ-donor, whereas a lower d/b ratio highlights the greater NHC $\leftarrow$ metal π-back-donation. Interestingly, in the studies conducted by Ghosh, greater NHC $\leftarrow$ metal π-back-donation was observed in Pd−NHC complexes exhibiting lower d/b ratios ranging between 2.59 and 3.99[13,14] and Au−NHC complexes with d/b ratios ranging between 5.23 and 5.88[15,16] compared with the Ag−NHC complexes with d/b ratios ranging between 7.8 and 12.68.[11,12,16] This observation could attest to why silver−NHC complexes are particularly better transmetalating agents.

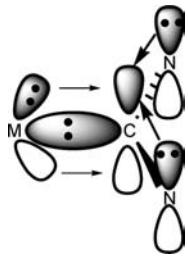

Figure 1. Orbital diagram of NHC bonding to metal center.

The newly emerging interest in the medicinal applications of stable metal−NHCs led us to examine the few accounts available in the literature dealing with this area of research. This review will discuss in detail the medicinal applications of various transition metal−NHC complexes including silver, gold, rhodium, ruthenium, and palladium. The antimicrobial, antitumor, and resistance properties, along with proposed mechanisms of action to suppress the bacterial growth or proliferation of tumor cells, will be discussed.

2. Imidazolium Salts as Antimicrobials

Before the evaluation of N-heterocyclic carbene−metal complexes as metallopharmaceuticals, an overview of the medicinal applications of imidazolium salt precursors is appropriate. Imidazolium salts are often used as precursors to metal−NHC complexes and are commonly one of the byproducts produced from the degradation of NHC−metal complexes. After a thorough search of the literature, it was evident that only a handful of groups have investigated the antimicrobial and antifungal properties of imidazolium salts in relation to various N-substituents. Pernak and co-workers examined a number of 3-alkylthiomethyl-1-ethylimidazolium chlorides **1a**−**f** (Chart 1).[22] The salts were synthesized by treating 1-ethylimidazole with the appropriate chloromethylalkyl sulfide in refluxing anhydrous benzene for 4 h. The products were isolated by extraction with hot hexanes affording hydroscopic oils with yields of 90%.

The antimicrobial activity was reported in terms of the minimum inhibitory concentration (MIC) values, which are defined as the lowest concentration of an antimicrobial that visibly inhibits the growth of the bacteria after an overnight incubation.[23] The antimicrobial activity was evaluated against *Staphylococcus aureus*, *Gaffkya tetragena*, *Sarcina lutea*, *Klebsiella pneumoniae*, *Serratia, marcescens*, *Rhodothorula glutinis*, and *Bacillus subtilis*. The results are summarized in Table 1.

The antimicrobial activity was determined in relation to the hydrophobicity of the imidazolium salts bearing the different alkyl substituents. It was found that the activity was related to the length of the alkyl chain with **1d** and **1e** showing the best response relative to their analogues. The MIC values in terms of micrograms per milliliters equate to 1.13−11.9 μg/mL for **1d** and 0.69−46 μg/mL for **1e**. It is important to point out that the results in Table 1 indicate that alkyl chain substituents adversely influence the antimicrobial activity of the imidazolium salts if they are too short or too long.

Further, Pernak investigated a series of 3-alkoxymethyl-1-methylimidazolium salts (Chart 1) with the effects of three different anions, Cl^-, BF_4^-, and PF_6^-.[24] Twelve different complexes were made for each anion, **2a**−**l** (Cl^-), **3a**−**l** (BF_4^-), and **4a**−**l** (PF_6^-) (Table 2). The MIC and the minimum bactericidal or fungicidal concentration (MBC) values were determined against the bacterial strains *Micrococcus luteus*, *Staph. epidermidis*, *Staph. aureus*, methicillin-resistant *Staph. aureus* (MRSA), *Entercoccus hirae*, *Escherichia coli*, *Proteus vulgaris*, *K. pneumoniae*, and *Pseudomonas aeruginosa*, and the fungal strains *Candida albicans* and *Rhodotorula rubra* (results not shown). The terms bactericidal and fungicidal indicate that the test compound kills the tested bacteria and fungi, respectively.

Chart 1. Structure of 3-Alkylthiomethyl-1-ethylimidazolium Chlorides 1a−f[22] and 3-Alkoxymethyl-1-methylimidazolium salts 2a−l, 3a−l, and 4a−l[24]

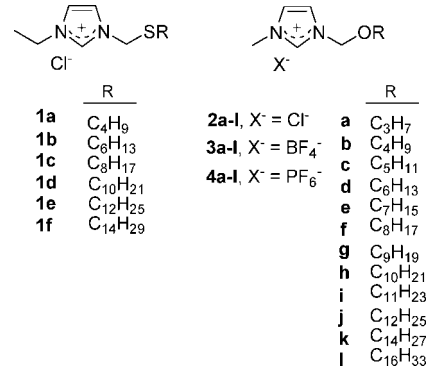

Although it was shown that the salts did possess antibacterial and antifungal activities, their efficacy depended greatly on the length of the alkyl chain. The type of anion did not exert any notable effect on the activity of the salts. The most active compounds against most bacterial strains were **2**−**4h**, **2**−**4i**, **2**−**4j**, and **2**−**4k**, bearing 10, 11, 12, and 14 carbon atoms, respectively, with the dodecyloxymethyl group as the most effective with MIC values ranging between 25 and 395 μM. This range equates to approximately 7.9−125 μg/mL. There was a general increase in the activity with increasing chain length against the fungal strains tested.

Additional studies done by Cetinkaya verified the same trends as observed earlier.[25] They explored the effects of lipophilic substituents, anions, and backbone substituents on the antimicrobial activity associated with a series of 1,3-diazolidinium salts (**5**) and the effect of ring size of pyrimidinium salts (**6**) as a comparison (Chart 2). The complexes were tested against a number of bacterial organisms, including *E. coli*, *Staph. epidermidis*, *Staph. aureus*, *Enterococcus faecalis*, *Enterobacter cloacae*, and *P. aeruginosa*, and *C. albicans* and were compared with ampicillin, a β-lactam antibiotic used to treat general bacterial infections.

The most notable feature observed among 30 derivatives synthesized is the remarkable enhancement of the antimicrobial activity against Gram-negative and Gram-positive bacteria of three derivatives of **5** by the addition of two mesityl or two mesitylmethyl substituents on both nitrogen atoms (bulky and lipophilic groups). Variation of the counterion of the imidazolidinium salt of **5**, with R_1 and R_3 as mesitylmethyl, greatly affected its antimicrobial activity. The mesitylmethyl derivative of **5** showed more effectiveness, especially with $X^- = Cl^-$ than its counterparts with MIC values of 3.12 μg/mL against *Staph. aureus*, *Ec. faecalis*, and *P. aeruginosa* and 6.25 μg/mL against *Staph. epidermidis*. The same derivative completely lost its activity when X^- was changed to PF_6^- or BF_4^-. Furthermore, variations to the backbone such as substitutions from hydrogens to methyl, cyclohexyl, or benzene groups were determined to decrease the activity of the NHC salts. Lastly, the antimicrobial activity of several derivatives of **5** was

Downloaded by UNIV MAASTRICHT on August 28, 2009 | http://pubs.acs.org
Publication Date (Web): July 6, 2009 | doi: 10.1021/cr800500u

Table 1. The Minimum Inhibitory Concentration log(1/MIC) for Complexes 1a−f[22]

	log(1/MIC)[a]						
compound	*Staph. aureus*	*G. tetragena*	*Sa. lutea*	*K. pneumoniae*	*Se. marcescens*	*R. glutinis*	*B. Subtilis*
1a	4.05	3.50	3.52	2.82	2.20	3.85	3.35
1b	4.35	4.35	3.75	3.75	2.84	4.05	4.05
1c	4.69	5.05	4.69	4.39	3.79	5.00	4.39
1d	5.12	5.45	5.12	4.99	5.12	5.12	4.43
1e	5.08	5.70	5.39	5.08	3.87	5.08	4.47
1f	4.83	5.27	5.13	4.75	3.95	4.93	4.49

[a] MIC results are based on 24 h incubation @ 37 °C. Values are expressed as mol/L.

Table 2. 3-Alkoxymethyl-1-methylimidazolium Salts 2−4[24]

Cl^-		BF_4^-		PF_6^-	
no.	R	no.	R	no.	R
2a	C_3H_7	**3a**	C_3H_7	**4a**	C_3H_7
2b	C_4H_9	**3b**	C_4H_9	**4b**	C_4H_9
2c	C_5H_{11}	**3c**	C_5H_{11}	**4c**	C_5H_{11}
2d	C_6H_{13}	**3d**	C_6H_{13}	**4d**	C_6H_{13}
2e	C_7H_{15}	**3e**	C_7H_{15}	**4e**	C_7H_{15}
2f	C_8H_{17}	**3f**	C_8H_{17}	**4f**	C_8H_{17}
2g	C_9H_{19}	**3g**	C_9H_{19}	**4g**	C_9H_{19}
2h	$C_{10}H_{21}$	**3h**	$C_{10}H_{21}$	**4h**	$C_{10}H_{21}$
2i	$C_{11}H_{23}$	**3i**	$C_{11}H_{23}$	**4i**	$C_{11}H_{23}$
2j	$C_{12}H_{25}$	**3j**	$C_{12}H_{25}$	**4j**	$C_{12}H_{25}$
2k	$C_{14}H_{29}$	**3k**	$C_{14}H_{29}$	**4k**	$C_{14}H_{29}$
2l	$C_{16}H_{33}$	**3l**	$C_{16}H_{33}$	**4l**	$C_{16}H_{33}$

Chart 2. Structures of 1,3-Diazolidinium Salts (5) and Pyrimidinium Salts (6)[25]

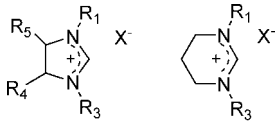

Chart 3. Structures of 1-Alkyl-2-methylimidazolium Complexes 7a−7f[26]

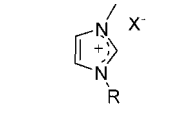

	R	X^-
7a	C_8H_{17}	Br^-
7b	$C_{10}H_{21}$	Cl^-
7c	$C_{12}H_{25}$	Br^-
7d	$C_{14}H_{29}$	Cl^-
7e	$C_{14}H_{29}$	Br^-
7f	$C_{16}H_{33}$	Br^-

directly compared with that of **6** with identical substituents, and it was established that the ring size plays a crucial role. The imidazolidinium salts were much more active than the pyrimidinium salts. The mechanism of activity of these complexes has not been studied, but it is thought that lipophilic side chains can disrupt intermolecular interactions and thus cause the dissociation of cellular membrane bilayers of the bacterial cell, which compromises cellular permeability and induces leakage of cellular contents.[26]

More recently Huen Lee and his group synthesized a series of quaternary imidazolium salts (**7a−f**) among others and tested their antimicrobial activity.[26] The general structure is shown in Chart 3. The salts were obtained by the deprotonation of the imidazole starting material with sodium or sodium ethanoate and the subsequent alkylation with the appropriate alkyl bromide or chloride in refluxing methanol or acetonitrile.

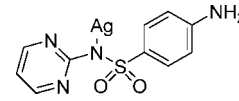

Figure 2. Structure of silver sulfadiazine.

The antimicrobial efficacy of the compounds was determined against *Bac. subtillis*, *Staph. aureus*, resistant *Staph. aureus*, *E. coli*, and *Salmonella typhimurium* bacterial strains plus *C. albicans* fungal strain. The preferred carbon chain lengths that produced the most efficient antimicrobial activity are **7c−f** with MIC values ranging between 4 and 8 μg/mL for most of the bacterial strains tested. Generally, as can be deduced from the various experiments that were described above, hydrophobic alkyl substituents such as long alkyl chains or sterically bulky groups have demonstrated their enhancement of the antimicrobial activity of imidazolium salts.

3. Silver

3.1. Medical Uses of Silver Compounds

Silver has been recognized as an effective antimicrobial agent, specifically in the form of silver nitrate since the 17th and 18th centuries.[27] The popularity of silver nitrate led to its utilization as a treatment of chronic skin ulcers, open wounds, and suppurating wounds well into the early 19th century.[28] Soon after the astringent properties of silver against a wide range of bacteria were recognized, a German obstetrician, C.F. Crede, introduced a prophylactic 2% silver nitrate eye solution to prevent ophthalmia neonatorum in newborns in 1880.[27] The emergence of penicillin and other antibiotics after World War II led to the abandonment of silver-based antimicrobials.[27] Shortly thereafter, resistant organisms such as *P. aeruginosa*, *Proteus mirabilis*, and *Proteus morgani* surfaced and led to the revival of silver nitrate by Moyer in 1965.[29] As a result, silver sulfadiazine (Figure 2) was introduced by Fox in 1968,[30] and it remains one of the most effective and widely used topical burn treatments.[31−33]

3.1.1. Mechanism of Silver Activity

Although the cytotoxic effects of silver against Gram-positive and Gram-negative bacteria have long been established, the mechanisms of action are not completely understood. Sporadic studies of the cell toxicity mechanisms of silver suggest that silver ions kill organisms through a variety of ways. Two excellent reviews by Lansdown and Hugo discuss the antimicrobial properties and the mechanism of action of silver.[34,35]

Briefly, studies done by Feng and co-workers suggest that treatment of *E. coli* and *Staph. aureus* with Ag^+ causes significant morphological changes in the bacterial cells as

Downloaded by UNIV MAASTRICHT on August 28, 2009 | http://pubs.acs.org
Publication Date (Web): July 6, 2009 | doi: 10.1021/cr800500u

Scheme 1. Synthesis of 8a, 8b, 9a, and 9b[63]

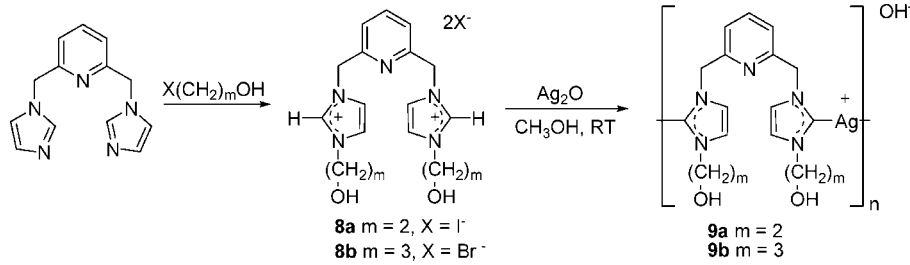

observed by transmission electron microscopy (TEM) and X-ray microanalysis.[36] Silver-treated cells exhibited an electron-light region in their cytoplasm with condensed DNA molecules. Condensed DNA molecules lose their ability to replicate. Electron-dense granules were detected around the cell wall inside the cytoplasm, and the cytoplasmic membrane experienced shrinkage and detachment from the cell wall thereafter. Furthermore, X-ray microanalysis of the electron-dense granules revealed the presence of silver and sulfur. This was an indication that silver ions interact with thiol groups leading to the deactivation of enzymatic proteins.

Another proposed mechanism by Fox and Modak suggested that the silver moiety in silver sulfadiazine dissociated from sulfadiazine and became bound to components within the cell. The subsequent inhibition of bacterial growth was attributed to the amount of silver bound to bacterial DNA.[37] The role of each component was determined using radioactive silver sulfadiazine (^{110}AgSD) and radioactive sulfadiazine (^{35}SD). It was established that the amount of SD entering the cell was not significant, and it is thus unlikely for the bacterial inhibition to be attributed to the SD moiety of AgSD. Furthermore, based on an *in vivo* model of *Pseudomonas* infected mice, silver seemed to function best if paired with sulfadiazine. AgSD had superior activity over other silver compounds perhaps due to the slow dissociation of the complex and thus continual release of Ag^+ over time.[38]

In addition, several groups investigated the effect of Ag^+ ions on the respiratory electron chain of *E. coli*.[39−41] Their studies lead to the conclusion that Ag^+ ions are highly toxic to microorganisms due to inhibition of the respiratory chain at multiple sites.

3.1.2. Toxicity of Silver

Although silver is generally nontoxic to humans, it is widely known that a prolonged and excessive exposure to silver causes the development of a rare and irreversible pigmentation of the skin (argyria), the eyes (argyrosis), or both. This is a characteristic blue-black discoloration formed by the interaction of silver ions with melanin and proteins in the wound exudates to give silver sulfide.[42] Argyria occurs after the topical application of silver compounds to wounds (localized argyria) or when silver is taken orally, injected directly into the blood stream, inhaled, or applied to mucosal surfaces (generalized argyria).[43] In the case of the latter, silver is absorbed and carried to different parts of the body where it is deposited, most commonly, in the eyes, internal organs, and sun-exposed body parts such as hand, arms, face, nails, etc.[43]

Several forms of silver are thought to cause argyria. Extended use of colloidal silver proteins, which have been used as allergy and cold medications and for a number of other ailments, can cause generalized argyria.[43] Colloidal silver proteins are metallic silver particles suspended in a polymer protein solution. Also, the use of antismoking tablets and gum, which contain silver acetate, have been reported to cause generalized argyria.[43,44] Several reports of localized and generalized argyria surfaced after the use of topical solutions of silver nitrate[45] and silver sulfadiazine cream.[43] It is important to note that argyria is rarely the cause of any ill effect or death and that there are no effective treatments for removing silver deposits from the body.[46] This can be explained by the fact that silver sulfide is highly insoluble with a K_{sp} of 10^{-50}.

Besides argyria, other toxic effects of silver may include upper and lower respiratory tract irritation. Based on some studies, these effects could be a result of the carrier molecule or anion such as the nitrate in some silver-based compounds rather than the silver itself.[47] Other effects involve the accumulation and binding of silver ions to reduced glutathione in the liver and directing it to the bile.[48] Reduction in glutathione concentrations could be of concern considering its role in preventing damage to red blood cells by neutralizing the toxic chemicals that enter the body. Although silver accumulation has been reported in a number of different tissues and internal organs throughout the body, only a few cases of silver toxicity have been presented. Some studies reported that silver was toxic in isolated cells, such as lymphocytes,[49] keratinocytes,[50] hepatocytes,[51,52] and fibroblasts[53] by inhibition of proliferation. Similarly, cases involving nephrotoxic syndrome[54] and leucopenia[55,56] have been reported in patients with severe burns treated with silver sulfadiazine. Other studies have shown that silver is virtually nontoxic. The issue of silver toxicity is still under debate, but ultimately, silver is known to be one of the least toxic metals.

3.1.3. Resistance to Silver

Silver is considered a broad-spectrum antibiotic. Silver, unlike conventional organic-based antibiotics, is active against a wide range of Gram-positive and Gram-negative bacteria and targets multiple sites on or within the bacterial cell. The multifaceted mode of action of Ag^+ ions is a major contributor to the scarcity of reports of silver resistance despite its liberal use. It is worth mentioning however that silver resistance was reported as early as 1975 when McHugh described the emergence of a *Salmonella* silver-resistant strain, which caused the deaths of three patients at Massachusetts General Hospital burn unit.[57] Since then, this area has been intensely researched and the underlying molecular basis is presently much more established.[58,59]

Silver and co-workers provided a detailed report of the genetic makeup of a 180 kb pMG101 plasmid isolated from a silver-resistant *Salmonella* strain.[60] The silver-resistant region within the plasmid was cloned and sequenced and was found to contain nine genes, two of which have unknown functions. The remaining seven genes are as follows: *silE*

Downloaded by UNIV MAASTRICHT on August 28, 2009 | http://pubs.acs.org
Publication Date (Web): July 6, 2009 | doi: 10.1021/cr800500u

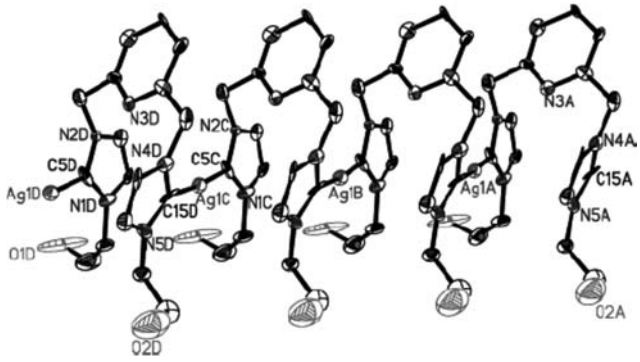

Figure 3. Molecular structure of **9a**.[63]

Table 3. MIC of 9a, 9b, and $AgNO_3$[63]

		E. coli		*P. aeruginosa*		*Staph. aureus*	
Test compd	Ag (mg/mL)	day 1	day 2	day 1	day 2	day 1	day 2
9a	1186	−	−	−	−	−	−
1DF		−	+	−	−	−	+
2DF		−	+	−	+	+	
3DF		+		+		+	
4DF		+		+		+	
9b	1125	−	−	−	−	−	−
1DF		−	+	−	+	−	+
2DF		−	+	−	+	−	
3DF		+		+		+	
4DF		+		+		+	
$AgNO_3$	3176	−	+	−	+	+	
1DF		+		+		+	
2DF		+		+		+	
3DF		+		+		+	
4DF		+		+		+	

DF = dilution factor; + = growth; − = no growth.

encodes a 143-amino-acid, periplasmic, Ag^+-specific metal-binding protein (SilE). This protein contains ten histidine residues that bind five Ag^+ cations. Upstream of the *silE* gene is the gene pair, *silRS*. This pair consists of a membrane kinase sensor (SilS) and a regulatory responder protein (SilR). This is followed by the *silCBA* genes, which determine a three-polypeptide cation/proton exchange complex that is potential-driven. The components of this efflux system are SilA, which forms a pathway for Ag^+ ions from the cytoplasm to the outer membrane protein, SilC, and finally SilB, the membrane fusion protein whose function is to maintain physical contact between SilA and SilC. Lastly, SilP, the last member of the silver-resistant determinant is a member of the heavy-metal resistance efflux P-type ATPase family. The unique silver-resistant determinant described above consists of two metal ion efflux pumps, SilCBA (the three-component cation/proton exchange complex) and SilP (the P-type ATPase), as well as SilE (the periplasmic metal-binding protein). A more thorough review of the molecular biology of bacterial silver resistance is provided by Silver.[61]

3.2. Antimicrobial Properties of Silver−NHC Complexes

For a review on the recent progress in the synthetic methods available for silver−NHC complexes, comprehensive structural analysis, and a detailed look at the uses of silver−NHCs as transfer agents, potential antimicrobials, and catalysts, the reader is directed to the recent contribution by Garrison and Youngs.[62]

Scheme 2. Synthesis of 10 and 11[64]

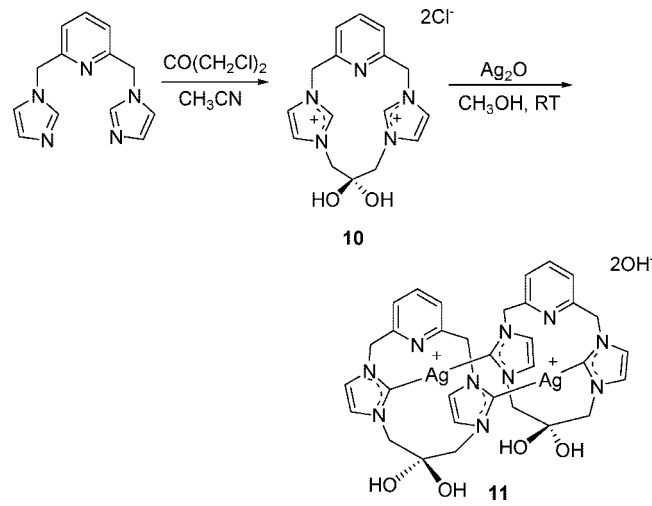

3.2.1. Synthesis and Antimicrobial Properties of Pyridine-Linked Pincer Silver−NHC Complexes

The first Ag(I)−NHC complexes possessing antimicrobial activity against *E. coli*, *Staph. aureus*, and *P. aeruginosa* were reported by Youngs in 2004.[63] The pincer ligands (**8a**, **8b**) were prepared by the reaction of 2,6-bis(imidazolemethyl)pyridine with 2-iodoethanol or 3-bromopropanol, respectively. The corresponding silver complexes **9a** and **9b** were readily obtained by the reaction of **8a** and **8b** with Ag_2O in aqueous methanol or water (Scheme 1).

The formation of (**9a**, **9b**) was confirmed by the disappearance of key resonance peaks at 9.13 ppm and 9.36 ppm associated with the imidazolium protons in the ^1H NMR spectra of **8a** and **8b**, respectively, and the appearance of a resonance at ca. 181 ppm in the ^{13}C NMR spectra corresponding to the formation of a C−Ag bond. Furthermore, the solid-state structure of **9a** illustrates the formation of a one-dimensional polymer with a nearly linear geometry at the Ag atom with a bond angle of 174.7(4)° (Figure 3).

The minimum inhibitory concentration (MIC) of **9a** and **9b** against a panel of pathogens, *E. coli*, *Staph. aureus*, and *P. aeruginosa*, was determined. $AgNO_3$ was used as a reference, and the corresponding salts **8a** and **8b** served as control. The results are summarized in Table 3. The silver complexes were dissolved in Luria broth (LB) culture medium, upon which a precipitate formed, presumably AgCl, and the solution was filtered. Serial dilutions of the silver complex−LB broth mixtures were prepared, and a volume of 20 μL of freshly grown organisms was added daily.

As shown in Table 3, **9a** and **9b** exhibited better bacteriostatic activity, even at much lower concentrations, compared with $AgNO_3$. This could be attributed to the fact that the pincer ligands stabilize their corresponding silver complexes to a certain extent, thereby controlling the release of the Ag^+ in the culture medium. $AgNO_3$ on the other hand could precipitate as the insoluble AgCl salt, thus reducing the concentration of the biologically active Ag^+ in the media. In turn, the active Ag^+ species in $AgNO_3$ is eventually consumed by the Cl^- adduct, whereas the Ag^+ species in both silver complexes **9a** and **9b** are released at a much slower rate and keep exerting their antimicrobial effects until consumed.

Another NHC cyclophane *gem*-diol salt was prepared by the reaction of 2,6-bis(imidazolemethyl)pyridine with 1,3-dichloroacetone.[64] The reaction appeared to proceed via an

Downloaded by UNIV MAASTRICHT on August 28, 2009 | http://pubs.acs.org
Publication Date (Web): July 6, 2009 | doi: 10.1021/cr800500u

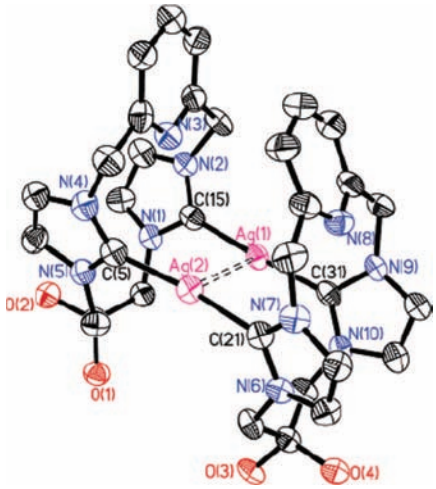

Figure 4. Molecular Structure of **11**.[64]

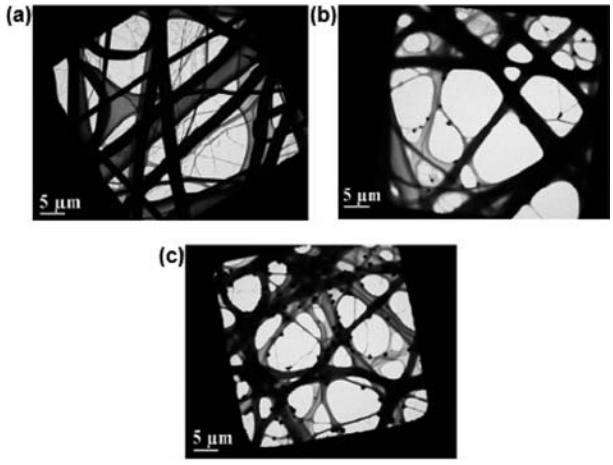

Figure 5. TEM image of the encapsulated complex **11** in Tecophilic polymer fiber mat showing deposition of silver ions over time: (a) electrospun fiber; (b) fiber after exposure to water vapor for 30 min; (c) fiber after exposure to water vapor for 65 h.[64]

acid-catalyzed process to yield (**10**). A subsequent reaction with Ag_2O yielded the corresponding silver complex (**11**) in good yield (Scheme 2). The formation of **11** was verified using NMR spectroscopy, which confirmed the loss of the imidazolium proton at 9.35 ppm in the ^{1}H NMR and the appearance of an apparent doublet in the ^{13}C NMR spectrum at 184−186 ppm. This resonance is presumably due to the coupling between the carbene carbon of **11** and ^{109}Ag and ^{107}Ag nuclei. Furthermore, the X-ray crystal structure shown in Figure 4 confirmed the formation of **11**.

In this report, a new method to ensure the slow release of silver ions was employed. Complex **11** was encapsulated into a medical grade polymer, Tecophilic, capable of absorbing up to 150% of its dry weight in water content. This feature is important for two reasons, both of which are essential for optimal wound healing. First, in the event of applying this silver encapsulated hydrophilic polymer to a wound site, the water content will allow for the release of silver ions from the polymer matrix. Second, the Techophilic will maintain a moist environment at the wound site, thereby accelerating the healing process. Besides its exceptional hydrophilic properties, Techophilic polymer is ethanol soluble, which made it feasible to electrospin both the polymer and silver complex **11** together to achieve a homogeneous mixing of the as-spun fiber.

Scheme 3. Synthesis of 12 and 13[66]

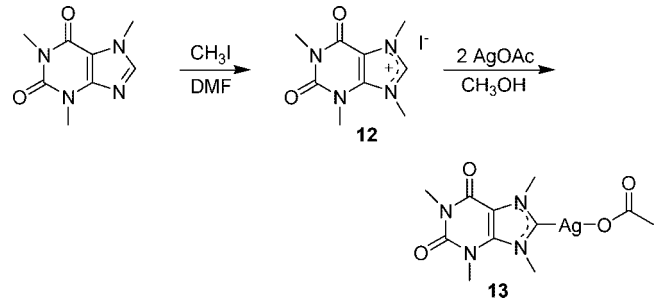

Table 4. MIC of 12[66]

species name	MIC (mg/mL)
P. aeruginosa	50
E. coli	50
Staph. aureus	100
C. albicans	150
A. niger	75
Sac. cerevisiae	150

The electrospun fibers were obtained by creating an electrically charged jet of solution containing the Techophilic polymer/complex **11** mixture. This method can produce fiber mats that range from a few nanometers to several micrometers in diameter.[65] Furthermore, TEM was used to characterize the resulting fibers. It was found that exposing the silver encapsulated fibers to a humid environment for up to 65 h caused the slow decomposition of complex **11**, which released silver particles into the polymer matrix (Figure 5).

The antimicrobial properties of the silver encapsulated polymer mat were evaluated against bacterial pathogens *E. coli*, *Staph. aureus*, and *P. aeruginosa*. By comparing the bactericidal activity of complex **11**, $AgNO_3$, and the **11**/Techophilic fiber mat, it was revealed that after a 48 h incubation period, $AgNO_3$ (MIC of 433 μg/mL) showed a better antimicrobial activity than the unencapsulated complex **11** (MIC of 838 μg/mL). However, the **11**/Techophilic fiber mat with the least amount of silver at 140 μg/mL showed sustained release of silver ions and thus enhanced antimicrobial activity over a period of days. Furthermore, the encapsulated silver NHC fiber mats exhibited a faster kill rate with lower silver content ($[Ag^+] = 140$ μg/mL or 424 μg/mL) compared with silver sulfadiazine with $[Ag^+] = 3020$ μg/mL or 0.5% silver nitrate with $[Ag^+] = 3176$ μg/mL. This observation could be attributed to the greater surface area provided by the polymer mats, through which active silver species can be released. Ultimately the study showed that the bioavailability of active silver species can be increased through encapsulation of the silver−NHC into the polymer mat.

3.2.2. Synthesis and Antimicrobial Properties of Silver−NHC Complexes Derived from Xanthines

Further investigations of biologically active silver−NHC complexes led to the synthesis of a modified caffeine silver acetate complex.[66] This was of particular interest due to the use of a xanthine derivative, caffeine, as a carrier molecule that has low toxicity and is readily available. Xanthines are biologically relevant molecules that have been used medicinally as diuretics and central nervous system stimulants and to promote smooth muscle relaxation by inhibition of cyclic adenosine monophosphate (cAMP) phosphodiesterase.[67]

Downloaded by UNIV MAASTRICHT on August 28, 2009 | http://pubs.acs.org
Publication Date (Web): July 6, 2009 | doi: 10.1021/cr800500u

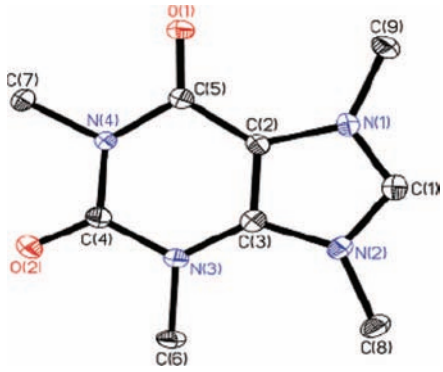

Figure 6. Molecular structure of the cationic portion of **12**.[66]

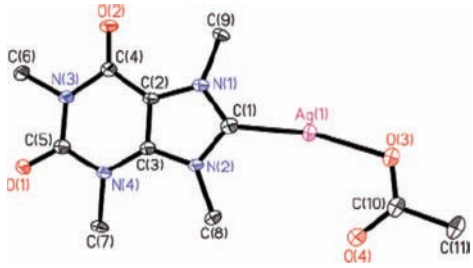

Figure 7. Molecular structure of **13**.[66]

Table 5. MIC of 13[66]

species (genomovar)	strain	MIC (μg/mL) M-H	MIC (μg/mL) LB
P. aeruginosa	27853-ATCC	4	10
	PAO1-V	4	4
	PA M57-15	2	4
	PA 2192	4	2
	PA 6294	6	6
	PA N6	1	10
	PA JG3	1	8
	PA N13	1	6
	PA 1061	1	8
	PA N8	1	6
	PA 324	1	6
	PA FRD1	1	10
B. cepacia (I)	PC783	6	6
B. multivorans (II)	HI2229	6	10
	AU8170	2	4
	AU5735	8	2
	AU7484	6	2
	AU5248	2	2
B. cenocepacia (III)	J2315	1	4
	HI2718	6	4
	ATTC BAA-245	1	4
B. stabilis (IV)	ATTC BAA-67	1	1
	HI2210	2	2
B. vietnamiensis (V)	PC259	4	4
B. dolosa (VI)	AU0645	4	8
	ATTC BAA-246	1	4
	AU4459	6	4
	AU5404	6	6
	AU4881	1	4
	AU9248	1	2
	AU4894	1	4
B. ambifaria (VII)	HI2468	6	6
B. anthina (VIII)	AU1293	4	4
B. pyrocinia (IX)	BC11	4	4
E. coli	J53	1	4
	J53 + pMG101	>5000	>5000

The methylated caffeine derivative (**12**) was synthesized by the reaction of caffeine with an excess of methyl iodide in DMF (Scheme 3). The formation of the water-soluble and air-stable imidazolium salt was confirmed by ^{1}H NMR, in which the imidazolium proton appeared at 9.30 ppm, and by ^{13}C NMR, in which the imidazolium carbon appeared at 139.6 ppm. The crystal structure of **12** is shown in Figure 6.

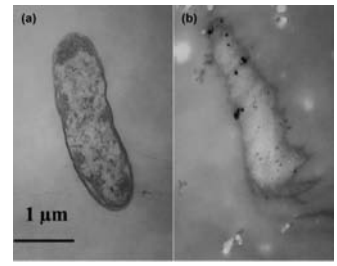

Figure 8. TEM of *B. dolosa* strain AU4459 of (a) normal cell and (b) cell treated with complex **13**.[66]

Scheme 4. Synthesis of 14 and 15[71]

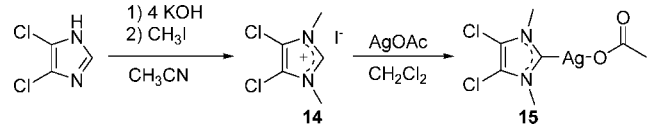

The subsequent formation of the silver acetate complex (**13**) was achieved via the *in situ* deprotonation of **12** with 2 mol equiv of silver acetate in methanol (Scheme 3). The disappearance of the resonance at 139.6 ppm corresponding to the imidazolium carbon of **12** in the ^{13}C NMR and the appearance of a characteristic resonance at 186.2 ppm corresponding to the carbene carbon atom further demonstrated the formation of **13**. The crystal structure of **13** is shown in Figure 7.

The antimicrobial activity of **12** against bacterial and fungal strains was studied (Table 4). It is not surprising that **12** exhibited some antimicrobial properties because caffeine has been known to induce mutations in bacteria and fungi by binding to DNA and interfering with normal cell cycle checkpoint functions.[68−70] Additionally, preliminary toxicity studies on a small number of Sprague Dawley rats showed that **12** exhibited very low toxicity (1.068 g/kg) when administered intravenously.

The *in vitro* antimicrobial activity of silver complex **13** was evaluated in detail against a panel of highly resistant pathogens recovered from the respiratory tract of cystic fibrosis (CF) patients (Table 5). In addition, *E. coli* J53 strains with and without the silver-resistant plasmid pMG101 were used as positive and negative controls in the MIC evaluation of **13**. The results demonstrated the efficacy of **13** against *E. coli* J53 lacking the pMG101 plasmid and the resistance of J53+pMG101 to **13** with MICs of <1 μg/mL and >5 μg/mL, respectively. The silver was the responsible moiety for the antimicrobial activity of complex **13**. Not only was complex **13** active against a number of bacterial strains, but it also showed a fungicidal effect on *Aspergillus niger* and *Saccharomyces cerevisiae*, with MIC values of 13 and 4 μg/mL, respectively, and fungistatic activity against *C. albicans* with a MIC value of 4 μg/mL.

In an attempt to understand the antimicrobial mechanism, a *Burkholderia dolosa* strain was treated with a 5 μg/mL dose of complex **13** for 1 h at 37 °C. TEM was used to evaluate the surface morphology of both the normal bacterial cell (Figure 8a) and the treated cell (Figure 8b) in LB medium. The treated cell showed major damage, which was characterized by cell "ghosts" completely lacking cytoplasm. The small dark clusters observed in the image (Figure 8b) were thought to be silver salts incorporated into the

Downloaded by UNIV MAASTRICHT on August 28, 2009 | http://pubs.acs.org
Publication Date (Web): July 6, 2009 | doi: 10.1021/cr800500u

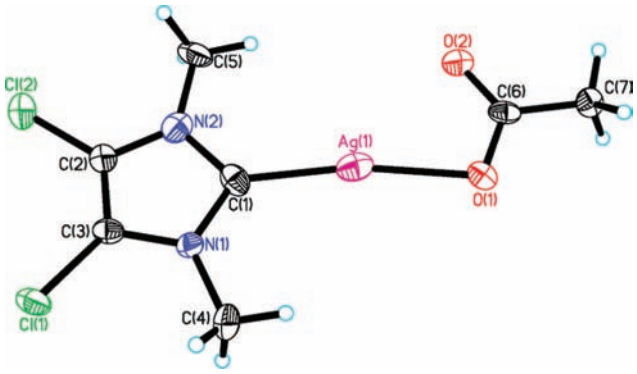

Figure 9. Molecular structure of **15**.[71]

Chart 4. Structures of 16 and 17[71]

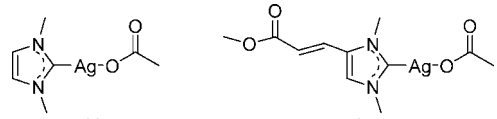

16 **17**

Table 6. Stability of Ag(I) Complexes 13, 15, 16, and 17[71]

silver complexes	stability in D_2O
13	3 d
15	17 weeks +
16	2 h
17	1.5 h

membrane of the treated cells. Those silver salts could be the cause of the apparent damage to the structural integrity of the cellular membrane.

3.2.3. Synthesis and Antimicrobial Properties of Silver−NHC Complexes Derived from 4,5-Dichloroimidazole

The Youngs group noted that complex **13** had stability in water for up to three days. It was hypothesized that the presence of electron-withdrawing substituents on the 4 and 5 positions of the imidazole ring may have helped to stabilize the silver complex from rapid degradation when exposed to water. Stable silver N-heterocyclic carbene complexes could play a very vital role in the systemic delivery of silver antimicrobials that could potentially reach and thereby treat infections prior to degradation by salts/biological molecules present in the blood stream. Keeping this in mind, a novel N-heterocyclic carbene derived from 4,5-dichloroimidazole was synthesized.[71]

The imidazolium salt 1,3-dimethyl-4,5-dichloroimidazolium iodide (**14**) was formed by the deprotonation of 4,5-dichloroimidazole with potassium hydroxide (KOH) and the subsequent methylation with iodomethane in acetonitrile (Scheme 4). Characterization using ^{1}H NMR spectroscopy revealed the presence of the imidazolium proton resonance at 9.42 ppm. In the ^{13}C NMR spectrum, the chemical shift at 136.6 ppm was consistent with the imidazolium carbon atom.

The formation of the corresponding silver complex (**15**) was achieved via the *in situ* deprotonation of **14** with 2 mol equiv of silver acetate in dichloromethane (Scheme 4). The most notable chemical shift at 179.7 ppm in the ^{13}C NMR spectrum denoted the carbene carbon atom of complex **15**, and it was within the typical range of other NHC−Ag(I) complexes. The solid-state molecular structure is shown in Figure 9.

To conduct a thorough investigation of the effect of NHC substituents on Ag−NHC stability, two similar Ag(I)−N-heterocyclic carbene complexes, one lacking any substituents on the 4 and 5 positions of the imidazole ring (**16**) and the second bearing a methyl ester group on the 4(5) position (**17**), were synthesized (Chart 4). Both complexes were synthesized by the general procedure of making the imidazolium iodide salt using iodomethane and the subsequent synthesis of the corresponding silver complex by adding 2 mol equiv of silver acetate in dichloromethane.

A stability analysis of all three silver complexes, **15**, **16**, and **17**, was performed by monitoring the degradation of the complexes in D_2O over time by ^{1}H and ^{13}C NMR spectroscopy. The results revealed that the presence of Cl atoms improved the stability of the silver acetate complex **15** over its analogues (Table 6). It was postulated that the Cl atoms, acting as σ-withdrawers and π-donators, led to a reduction of σ-donor capability[72] thereby leaving the carbene carbon center with less electron density and, therefore, less susceptible to attack by protons present in an aqueous environment.

The MIC of silver complex **15** was evaluated against a panel of highly resistant respiratory pathogens, mainly strains of *P. aeruginosa* and *Burkholderia* species in two different growth media, Mueller−Hinton (M−H) and Luria broth (LB) (Table 7). In addition, *E. coli* J53 strain (silver-sensitive) and J53 + pMG101 strain (silver-resistant) were used as positive and negative controls in the MIC evaluation of **15**. The MBC was also evaluated for **15** and was found to depend on two factors, the growth media in which the tested strain was grown and the strain itself. Complex **15** seemed to have a better bactericidal activity in M−H broth against some of the tested strains, but only showed a bacteriostatic activity for other strains at the concentrations examined. As defined previously, the term bactericidal indicates that the compound kills the tested bacteria, while bacteriostatic indicates that the compound inhibits the growth of the bacteria but does not necessarily kill it. It has been demonstrated that **15** is bactericidal for numerous strains at clinically achievable concentrations (Table 7).

A comparative antimicrobial study with complexes **15** and **16** on representative strains of *P. aeruginosa* and *Burkholderia* species found that the MIC_{50} values were basically the same when compared on a molar basis. This result was irrespective of the difference in the rate of degradation between the two silver complexes, which was a further indication that the Ag^+ ions are the active moiety within any Ag(I)−NHC.

3.2.4. Synthesis and Antimicrobial Properties of Silver−NHC Complexes Derived from 1-Benzyl-3-tert-butylimidazole

Another important contribution by the Ghosh research group led to the synthesis and antimicrobial evaluation of an (NHC)AgCl complex (**18**), which exhibited significant antimicrobial activity.[73] Complex **18** was synthesized according to Scheme 5 where the 1-benzyl-3-*tert*-butylimidazolium chloride salt precursor was treated with half an equivalent of Ag_2O in dichloromethane. The formation of **18** was further demonstrated by the disappearance of the imidazolium proton resonance in the 10 ppm region in the

Downloaded by UNIV MAASTRICHT on August 28, 2009 | http://pubs.acs.org
Publication Date (Web): July 6, 2009 | doi: 10.1021/cr800500u

Table 7. MIC and MBC of 15[71]

species (genomovar)	strain	MIC (μg/mL) M−H	MIC (μg/mL) LB	MBC (μg/mL) M−H	MBC (μg/mL) LB
P. aeruginosa	PA O1-V	2	2	>10	>10
	PA M57-15	4	1	6	4
	PA 2192	1	2	4	>10
	PA 6294	2	2	>10	>10
	PA N6	1	2	4	>10
	PA JG3	2	2	4	8
	PA N13	1	2	10	4
	PA 1061	1	2	6	10
	PA N8	1	2	>10	>10
	PA 324	1	1	2	>10
B. cepacia (I)	PC783	1	4	2	8
B. multivorans (II)	HI2229	1	4	1	>10
	AU8170	4	4	*a*	*a*
	AU5735	2	2	*a*	*a*
	AU7484	2	2	*a*	*a*
	AU5248	4	2	*a*	*a*
B. cenocepacia (III)	J2315	2	1	4	>10
	HI2718	2	>10	2	>10
	ATTC BAA-245	2	2	*a*	*a*
B. stabilis (IV)	ATTC BAA-67	1	>10	6	>10
	HI2210	1	>10	2	>10
B. vietnamiensis (V)	PC259	1	1	6	>10
B. dolosa (VI)	AU0645	1	2	1	6
	ATTC BAA-246	1	2	4	6
	AU4459	1	1	4	6
	AU5404	1	2	*a*	*a*
	AU4298	2	2	*a*	*a*
	AU3556	1	2	*a*	*a*
	AU4881	4	4	*a*	*a*
	AU9248	4	2	*a*	*a*
	AU4894	4	2	*a*	*a*
	AU3123	4	2	*a*	*a*
	AU4750	4	2	*a*	*a*
B. ambifaria (VII)	HI2468	2	1	4	>10
B. anthina (VIII)	AU1293	1	2	1	4
B. pyrocinia (IX)	BC11	1	1	1	1
E. coli	J53	2	4	>10	>10
	J53 + pMG101	>10	>10	>10	>10

[a] Not determined.

Downloaded by UNIV MAASTRICHT on August 28, 2009 | http://pubs.acs.org
Publication Date (Web): July 6, 2009 | doi: 10.1021/cr800500u

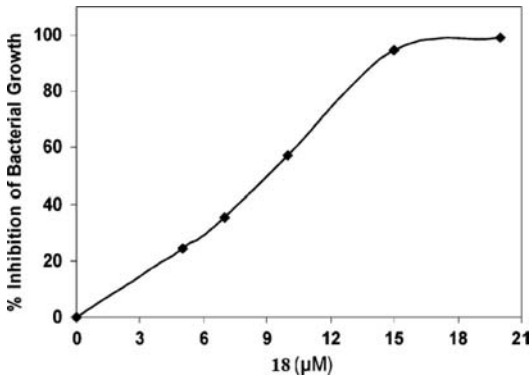

Figure 10. Percent inhibition of *Bac. subtilis* 168 cell proliferation by complex **18**.[73]

Scheme 5. Synthesis of 18[73]

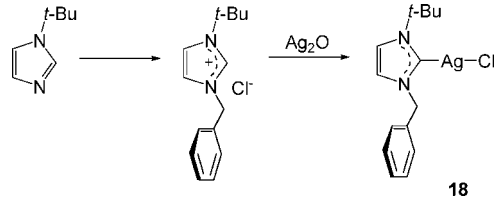

^{1}H NMR spectrum and the appearance of the N*C*N−Ag characteristic resonance at 177.7 ppm in the ^{13}C NMR spectrum.

Scheme 6. Synthesis of 19a, 19b, 20a, and 20b[74]

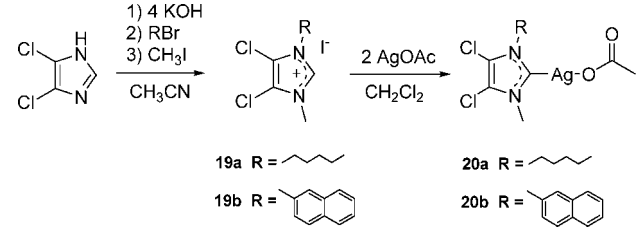

The antimicrobial activity of **18** against *Bac. subtilis* and *E. coli* was evaluated using different concentrations of **18** and measuring the bacterial growth at different time intervals.[73] The growth of the Gram-positive *Bac. subtilis* was inhibited as demonstrated by Figure 10, whereas no effect on the growth of the Gram-negative *E. coli* was observed. The antimicrobial activity of the 1-benzyl-3-*tert*-butylimidazolium chloride salt precursor was also evaluated, but no effect on the growth of the bacterial strains was noted, further demonstrating that the silver moiety of complex **18** was responsible for the reported activity. Furthermore, for the wild-type *Bac. subtilis* 168, the half-maximal inhibitory concentration (IC_{50}) and MIC for complex **18** were determined to be 9 ± 1.5 μM and 25 ± 3.2 μM, respectively.

Table 8. Half-Maximal Inhibitory Concentrations (IC_{50}) Measured Using the MTT Assay[74]

	IC_{50} (μM)[a]		
test compound	OVCAR-3	MB157	HeLa
15	35	8	>200
20a	30	20	>200
20b	20	10	>200
$AgNO_3$	35	5	50
AgOAc	20	12	*b*
cisplatin	12	25	25

[a] IC_{50} results are based on 72 h incubation period. [b] Not determined due to solubility limitations of AgOAc.

3.3. Antitumor Properties of Silver−NHC Complexes

3.3.1. Synthesis and Antitumor Properties of Silver−NHC Complexes Derived from 4,5-Dichloroimidazole

Several factors led the Youngs research group to test and report the efficacy of Ag(I)−NHC complexes **15**, **20a**, and **20b** against the human cancer cell lines OVCAR-3 (ovarian), MB157 (breast), and HeLa (cervical).[74] One of those factors was the urgent need to find new chemotherapeutic agents effective against cisplatin-resistant tumor cell lines with milder toxic effects. Another important factor was the current interest in other metal−N-heterocyclic carbene complexes demonstrating notable tumor cytotoxicity.[73,75,76] Furthermore, Ag(I)−phosphine complexes with antitumor activity were first reported by Sadler in 1988.[77] Since the start of this work, other reports of silver-based complexes possessing anticancer activity have appeared in the literature.[78−80]

Complexes (**20a**, **20b**) were synthesized according to Scheme 6. The 4,5-dichloroimidazolium iodide salt precursors (**19a**, **19b**) were synthesized by the deprotonation of 4,5-dichloroimidazole with KOH followed by the substitution with 1 equiv of the appropriate alkyl or aryl bromide in acetonitrile and subsequent methylation with an excess amount of iodomethane. Subsequent *in situ* deprotonation of **19a** and **19b** with silver acetate in a 1:2 molar ratio in dichloromethane afforded the corresponding NHC silver acetate complexes.

The *in vitro* efficacy of complexes **15**, **20a**, **20b**, the imidazolium cation precursors **14**, **19a**, and **19b**, silver nitrate, silver acetate, and cisplatin was determined against the human cancer cell lines OVCAR-3 (ovarian), MB157 (breast), and HeLa (cervical) using the MTT assay (Table 8). In the MTT assay, the enzyme succinate dehydrogenase present in the mitrochondria of living cells cleaves the tetrazolium rings of the yellow MTT to form insoluble purple formazan crystals. Sodium dodecyl sulfate (SDS) is a solubilizing solution added to dissolve the formazan. The absorbance of the resulting colored solution was measured at a wavelength of 570 nm. The number of surviving cells is directly proportional to the amount of formazan present.

The imidazolium salts **14**, **19a**, and **19b** showed much higher IC_{50} values and were therefore not active against the tumor cell lines tested (results not shown). As shown in Table 8, complexes **15**, **20a**, and **20b** were comparable in activity to cisplatin against OVCAR-3 and MB157 cell lines. However, the silver complexes showed minimal activity against HeLa cells. This was an indication that the reported silver complexes are selective in their preference against certain cancers.

The live/dead assay was used to measure cell viability. It is a two-color flourescent assay that simultanously determines the number of live cells as well as the number of dead cells. Live cells produced a red fluorescence due to their ability to metabolize C_{12}-resazurin, and dead cells produced a green fluorescence due to their compromised cell membranes allowing the accumulation of the Sytox Green stain. The images shown in Figure 11a−f represent fluorescence images from OVCAR-3 and MB157 control, incubation with cisplatin, and incubation with complex **15**.

Based on the quantitative measurements of the assay (Figure 12), the viability of OVCAR-3 cells exposed to silver complexes **15**, **20a**, and **20b** was 11%, 0%, and 0%, respectively. These results were superior to those for OVCAR-3 cells treated with cisplatin, which resulted in 78% viability. The OVCAR-3 control cells were 93% viable. Furthermore, all three silver complexes and cisplatin were equally active against MB157 cancer cell lines with 10% cell viability compared with the control cells, which exhibited 92% viability. The cell viability percent values were based on cell counts after incubation of the cells with the test compounds for 36 h at 50 μM. Cell viabilities were found to be significant using Tukey's multiple comparison among means ($\alpha = 0.05$).

The effect that silver imposed on the morphology of the OVCAR-3 and MB157 cells can be seen in Figure 13a−f in which the cells were incubated with complex **15** at 50 μM for 36 h. The cells were stained blue with Hoesch stain. The results were compared with the morphology of cisplatin-treated cells. Silver complex **15** had a considerable effect on the viability of the treated cells as compared with the control.

The *in vitro* results with the silver complexes **15**, **20a**, and **20b** showed excellent activity specifically against OVCAR-3 ovarian cancer cells and MB157 breast cancer cells. This sparked interest in the activity of these silver complexes *in vivo*. A preliminary study was conducted in which a small number of athymic nude mice were inoculated with 10^7 OVCAR-3 cells subcutaneously in their backs. The tumors were allowed to grow for approximately 6 weeks after which subcutaneous (SubQ) injections of silver complex **15** were performed along with control injections (diluent alone). One complex **15** dose group (333 mg/kg per injection) was SubQ injected every third day for 10 days. The total SubQ doses (~1000 mg/kg) were within the range of another parallel study where intraperitoneal (IP) injections (100 mg/kg per injection) were administered for 10 consecutive days. After day 10, all mice were humanely sacrificed. All dead mice underwent necropsy to evaluate the spleen size, evidence of gastrointestinal toxic effects, and the condition of the liver and kidneys along with the effect of **15** on the tumors. Figure 14 gives a view of the internal organs of one of the treated mice, in which all organs looked grossly normal. This result was further confirmed by a histopathological assessment of the brain, liver, lungs, heart, kidneys, and spleen. The tumors treated with silver, however, were determined to be necrotic, whereas the control tumors were still viable (Figure 15).

4. Gold

4.1. Medical Uses of Gold Compounds

The discovery of the bacteriostatic properties of gold cyanide, $K[Au(CN)_2]$, by Robert Koch in 1890 against tubercle bacillus marked the start of its use in modern medicine.[85,86] By 1920, the wide use of various gold salts as

Downloaded by UNIV MAASTRICHT on August 28, 2009 | http://pubs.acs.org
Publication Date (Web): July 6, 2009 | doi: 10.1021/cr800500u

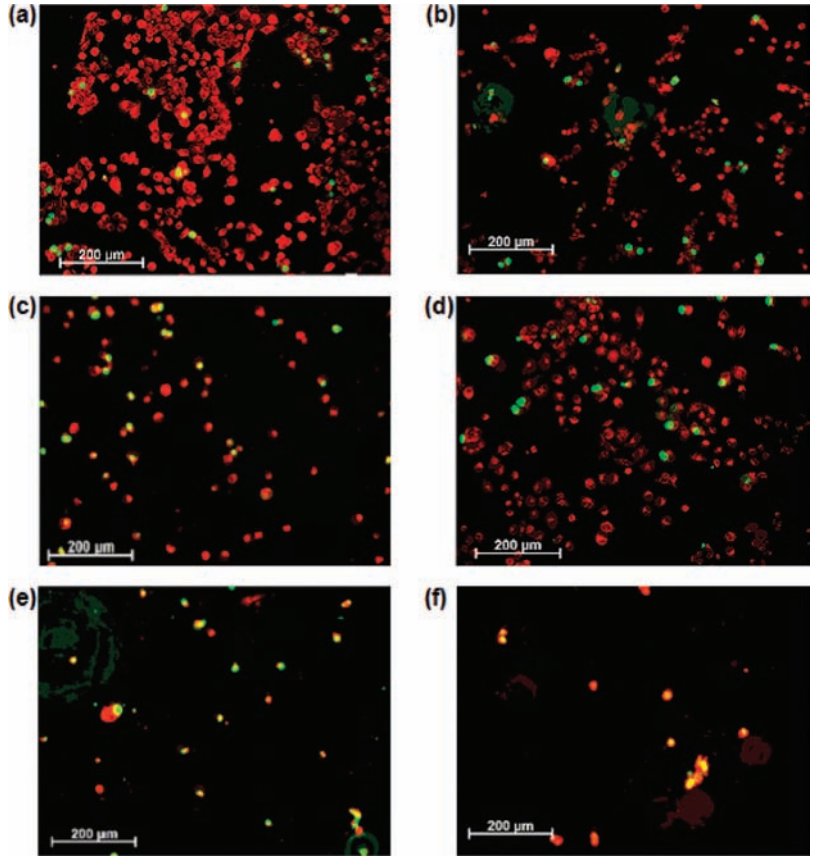

Figure 11. Live/dead assay images of OVCAR-3 and MB157 cells:[74] (a) OVCAR-3 control; (b) OVCAR-3 incubated with cisplatin; (c) OVCAR-3 incubated with **15**; (d) MB157 control; (e) MB157 incubated with cisplatin; (f) MB157 incubated with **15**.

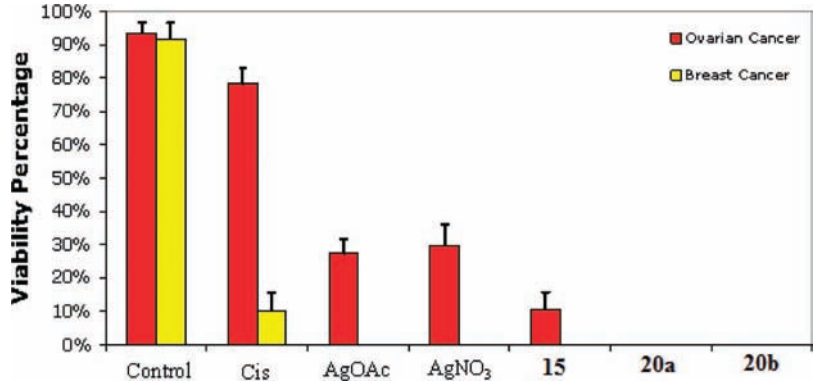

Figure 12. Percent viability of OVCAR-3 and MB157 after treatment with cisplatin (Cis), silver acetate, (AgOAc), silver nitrate ($AgNO_3$), **15**, **20a**, and **20b**. The percentages are based on cell counts from the live/dead assay data after incubation with test compounds at 50 μM for 36 h.[74]

a treatment for tuberculosis was underway. The belief that rheumatoid arthritis was an atypical form of tuberculosis led to the use of gold(I) salts for the treatment of this disease. By the early 1930s, gold therapy (chrysotherapy) was discontinued as a treatment of tuberculosis based on its ineffectiveness; however it is still considered the most effective available therapy for the management of rheumatoid arthritis.[87] No major therapeutic advancements have taken place in this field except for the antiarthritic gold compound auranofin (Figure 16), which was introduced in the early 1980s. Auranofin or triethylphosphine(2,3,4,6-tetra-*O*-acetyl-β-1-D-(thiopyranosato-S)gold(I) was introduced as an orally bioavailable drug designed in hopes of improving the pharmacokinetic profile, as well as reducing the cytotoxic effects (discussed in a later section), encountered with other gold compounds.[85−87]

Besides the antiarthritic applications of gold compounds, ophthalmologists use metallic gold to treat a condition called lagophthalmos, which is the inability to close the eyelids completely. This is done by surgically implanting metallic gold "weights" in the upper eyelid to help it close fully.[86]

The antimicrobial activity of gold compounds was investigated in light of the early evidence of their activity against tubercle bacillus presented by Robert Koch. Recent studies looked at the effect of a gold(I) thiocyanate complex, $Au(SCN)(PMe_3)$, against a number of Gram-positive bacterial strains including MRSA, methicillin-sensitive *Staph. aureus*, *Ec. faecalis*, coagulase-negative staphylococci, and streptococci.[81] The compound was mostly active against *Ec. faecalis* and *Staph. aureus* with MIC_{50} values of 0.77 and 0.33 μg/mL, respectively.[81] Furthermore, a comparative *in vitro* toxicity study against CHO mammalian cell lines demon-

Downloaded by UNIV MAASTRICHT on August 28, 2009 | http://pubs.acs.org
Publication Date (Web): July 6, 2009 | doi: 10.1021/cr800500u

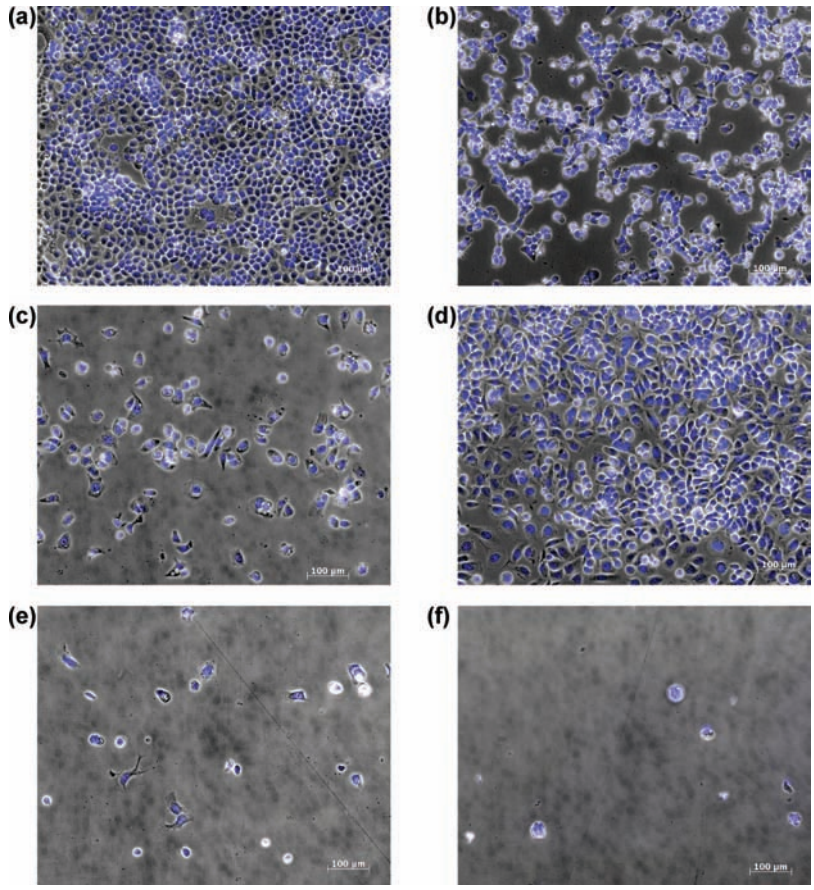

Figure 13. Morphology of OVCAR-3 and MB157 cells:[74] (a) OVCAR-3 control; (b) OVCAR-3 incubated with cisplatin; (c) OVCAR-3 incubated with **15**; (d) MB157 control; (e) MB157 incubated with cisplatin; (f) MB157 incubated with **15**.

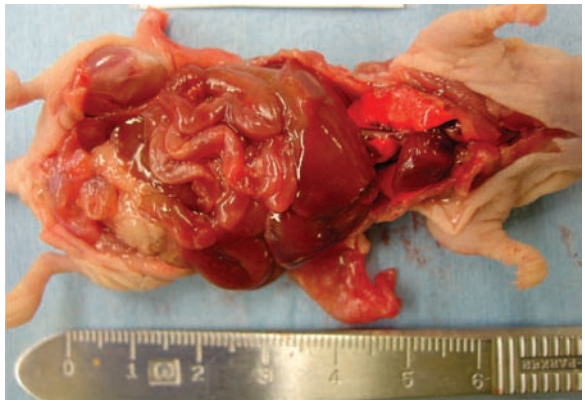

Figure 14. View of the internal organs of a mouse treated with three SubQ injections of complex **15** of 333 mg/kg dose over a 10 day period.[74]

strated the selectivity of the Au(I) thiocyanate complex for bacteria over mammalian cells with a MIC_{50} at least ten times greater than the bacterial MIC values.[81] A number of gold(III) compounds, namely, $AuCl_2$(damp) and $Au(OAc)_2$(damp), were also tested (Chart 5). Although both complexes were adequately active against Gram-positive bacteria and *E. coli*, the more water-soluble complex $Au(OAc)_2$(damp) showed enhanced selectivity against *Ec. faecalis* and *Staph. aureus*.[81]

Another major and current area of study involves the use of gold in the treatment of cancer. Auranofin was found to have a limited antitumor activity against HeLa cells (cervical cancer) *in vitro* and P388 leukemia cells *in vivo* but was inactive in solid tumors, which prompted the evaluation of other gold-based complexes. A number of triphenylphosphine gold(I) complexes were evaluated and have shown marked antitumor activity. For a comprehensive table, the reader is referred to a previous review in *Chemical Reviews* by Shaw.[87] The screening efforts of the different complexes led to the evaluation of a cationic tetrahedral gold(I) phosphine complex, $[Au(dppe)_2]Cl$ (Figure 17).[82] It is important to note that the bis(diphenylphosphino) ethane (dppe) ligand exhibits antitumor activity in itself, and it was suggested that the gold serves to protect it against degradation.[77,82] However, extensive studies done comparing the antitumor activity of dppe alone to $[Au(dppe)_2]Cl$ and other Au(I), Ag(I), and Cu(I) phenyl-substituted diphosphine complexes demonstrated that the antitumor activity was comparable, but the metal complexes were 20-fold more potent.[77,82] This result suggests that the effect of such metals expands beyond protection against degradation. Although the gold complex $[Au(dppe)_2]Cl$ exhibited excellent antitumor activity, it never made it to clinical trials due to the extensive cardiovascular toxicity unveiled during the preclinical toxicology studies.[83]

Similar cationic gold(I) phosphine complexes in which pyridyl groups replaced the phenyl substituents in $[Au(dppe)_2]Cl$ were synthesized for the purpose of evaluating the effects of decreased lipophilicity (Chart 6).[84] The presence of the pyridyl ligands and the position of the N atom introduce significant changes within the interactions between the compounds and the solvent. As evidence, the 4-pyridyl complex exists as a simple monomeric cation in the solid state and in solution. In contrast, the 2-pyridyl complex exists as a dimer in the solid state, and in solution, it exists in a constant equilibrium state between monomeric, dimeric, and tetrameric clusters. This further provides an explanation as

Downloaded by UNIV MAASTRICHT on August 28, 2009 | http://pubs.acs.org
Publication Date (Web): July 6, 2009 | doi: 10.1021/cr800500u

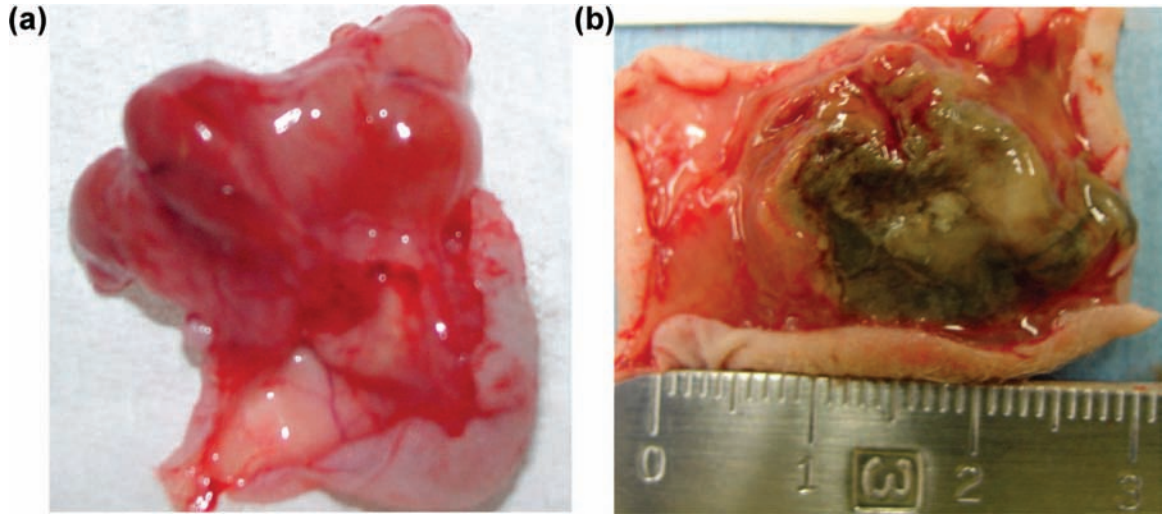

Figure 15. Image of the solid OVCAR-3 tumors allowed to grow in athymic nude mice: (a) healthy tumor before SubQ injection of complex **15**; (b) necrotic tumor after three SubQ injections of 333 mg/kg dose of **15** over a 10 day period.[74]

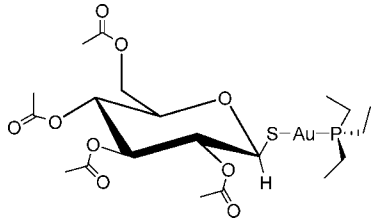

Figure 16. Structure of auranofin.

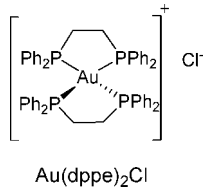

Au(dppe)$_2$Cl

Figure 17. Structure of antitumor Au(dppe)$_2$ chloride complex.

Chart 5. Structures of Antimicrobial Gold(III) Complexes

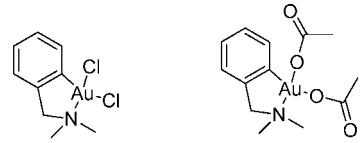

AuCl$_2$(damp) Au(OAc)$_2$(damp)

Chart 6. Structures of Antitumor Bis[1,2-bis(di-*n*-pyridylphosphino)ethane] Gold(I) Chloride Complexes Where $n = 2$ or 4

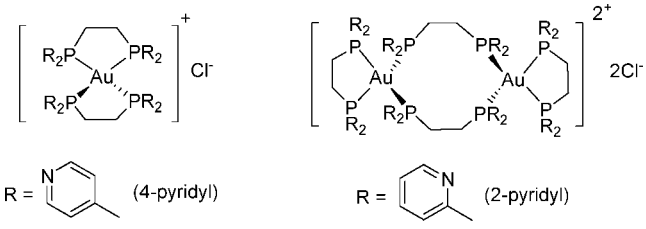

R = (4-pyridyl) R = (2-pyridyl)

to why the 4-pyridyl has much more water solubility than its analogue, the 2-pyridyl complex. It was found that the 2-pyridyl complex had a similar activity against P388 leukemia compared with [Au(dppe)$_2$]Cl, and it was also active against B16 melanoma *in vivo*. On the other hand, the 4-pyridyl complex was inactive against all tumor cell lines tested and was toxic to mice.

A dependence on lipophilicity was observed when the Au(I) complexes were tested *in vivo* against the murine colon 38 adenocarcinoma. The drugs were administered daily for 10 days. The compound with the intermediate lipophilicity, namely, the 2-pyridyl complex, showed the most antitumor activity, significant tumor growth delay of 9 days, decreased dose-limiting toxicity, and higher gold concentrations in the tumor. The most lipophilic, namely, [Au(dppe)$_2$]Cl, and the most hydrophilic, namely, the 4-pyridyl complex, had no marked effect on tumor growth delay. The lipophilicity factor was also used to explain the toxicity observed between the compounds mentioned. It is thought that very lipophilic aromatic cations such as [Au(dppe)$_2$]Cl exhibit high and nonspecific binding to proteins, which might explain the high host toxicity. In contrast, highly hydrophilic molecules such as the 4-pyridyl complex demonstrate low protein binding and high rates of excretion, which might explain its inactivity.

For more comprehensive reviews that address the early developments in the medicinal chemistry of gold complexes, the reader is directed to reviews by Fricker,[85] Merchant,[86] and Shaw.[87]

4.1.1. Mechanism of Gold Activity

Although gold has been used in the clinical setting for almost 80 years, its cytotoxic mechanisms are not completely understood. It has been established that gold complexes with different geometries exert their effect through different modes of action. For instance, the monomeric linear complex, auranofin, which is well-known for its antiarthritic properties, has the ability to undergo ligand exchange reactions where it displaces both of its ligands and forms different metabolites, one of which is [Au(CN)$_2$]$^-$, thought to target and inhibit certain immune cell functions involved in the inflammatory response of rheumatoid arthritis.[87] Auranofin, which was also found to exhibit antitumor activity,[88,89] was found to inhibit the growth of tumor cells via an antimitochondrial mechanism,[90,91] which involves the inhibition of mammalian selenoenzyme mitochondrial thioredoxin reductase (TrxR).[92,93] This is thought to occur through the binding of Au(I) to the C-terminal redox active -Cys-Sec- center.[94]

On the other hand, the cationic tetrahedral gold(I) phosphine complexes do not undergo ligand dissociation reactions due to the added stability by two chelating diphosphine

Downloaded by UNIV MAASTRICHT on August 28, 2009 | http://pubs.acs.org
Publication Date (Web): July 6, 2009 | doi: 10.1021/cr800500u

ligands. The stability of such complexes in the presence of thiols, disulfides, and serum proteins was assessed by monitoring ^{31}P NMR spectroscopy.[82] The ^{31}P NMR resonance was unaffected by the addition of glutathione (GSH and GSSH, thiol and disulfide sources) and after incubation with bovine serum. As judged by the NMR spectra, the gold phosphine complexes do not readily undergo ligand displacement reactions in the presence of thiols in aqueous media. This is perhaps a result of the high stability of the gold−phosphorus bonds.

Furthermore, it was recognized that the mitochondria might be a critical intracellular target involved in the antitumor activity of the drugs. Studies using isolated rat hepatocyte mitochondria were carried out in order to assess the effects exerted by $[Au(dppe)_2]Cl$ complex.[84] The cationic and lipophilic nature of this particular complex could have aided its uptake into the mitochondria. Once there, $[Au(dppe)_2]Cl$ is thought to cause a number of crucial modifications to the mitochondria including loss of the inner membrane potential difference, efflux of Ca^{2+}, increased mitochondrial respiration, mitochondrial swelling, and finally increased permeability of the inner mitochondrial membrane and uncoupling of oxidative phosphorylation.[90] These effects are thought to be particular to the lipophilic nature of $[Au(dppe)_2]^+$ and other tetrahedral bis(dipyridylphosphino)gold(I) complexes. This property could play an important role in improving the selectivity of the mitochondrial-targeted drugs by fine-tuning their degree of liphophilicity.

For a more comprehensive review of this topic, the reader is directed to two excellent reviews by Berners-Price that address the possible role of mitochondria in the mechanisms of cytotoxicity and antitumor activity of gold complexes,[90] as well as the recent strategies on specifically targeting the mitochondrial cell death pathway with gold compounds.[93]

4.1.2. Toxicity of Gold

Although the $[Au(dppe)_2]Cl$ complex has shown *in vivo* activity against P388 leukemia, M5078 reticulum cell sarcoma, B16 melanoma, mammary adenocarcinoma 16/C, and intraperitoneal and subcutaneous transplanted tumors, it was determined that this complex was severely hepatotoxic upon the *in vivo* evaluation in male beagle dogs.[90] As mentioned above, this $[Au(dppe)_2]Cl$ -induced cytotoxicity to liver cells could be a direct effect of its ability to cause the uncoupling of oxidative phosphorylation, which is related to the increased permeability of the inner mitochondrial membrane.[90]

Normal cells rely on oxygen consumption and oxidative phosphorylation for ATP production, whereas solid tumors have been shown to rely primarily on glucose uptake and glycolysis for ATP production. Therefore, antitumor agents that target the oxidative phosphorylation pathways (i.e., $[Au(dppe)_2]Cl$) are likely to cause toxicity in normal cells.[90] The pronounced difference between normal tissues and solid tumors related to their reliance on oxidative phosphorylation vs glycolysis for ATP production can be utilized in order to design selective and therefore effective antitumor agents.

4.2. Antimicrobial Properties of Gold−NHC Complexes

For a review on the recent progress in the synthetic methods available for gold−NHC complexes, their medicinal applications, and theoretical calculations that accompanied many synthetic studies, the reader is directed to the recent contribution by Cronje and Raubenheimer.[95]

Scheme 7. Synthesis of 21−26[98]

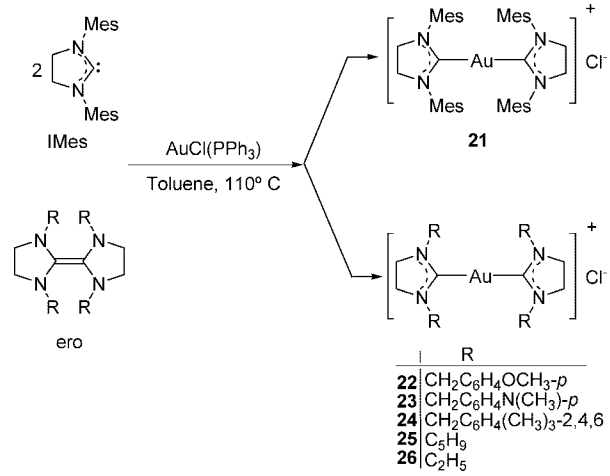

4.2.1. Synthesis and Antimicrobial Properties of Gold−NHC Complexes Derived from 1,3-Diorganylimidazolidin-2-ylidenes

As discussed previously, two-coordinate gold(I) phosphine complexes were reported to have potent antimicrobial activity.[85,96,97] However, Cetinkaya was the first to report the antimicrobial activity of six gold(I)−NHC complexes (**21**−**26**).[98] The gold−carbene complexes were synthesized following a general and simple procedure. The synthesis was carried out under argon or nitrogen atmosphere by reacting 1 equiv of $AuCl(PPh)_3$ with either 2 equiv of 1,3-dimesitylimidazolidin-2-ylidene (**21**) or equal equivalents of the corresponding bis(1,3-dialkylimidazolidin-2-ylidene) (**22**−**26**) (Scheme 7). The reaction mixtures were refluxed in toluene for 2 h and then cooled to room temperature where hexanes were added to obtain a creamy solid, which was recrystallized from a CH_2Cl_2/Et_2O mixture. The resulting gold complexes (**21**−**26**) were analyzed and confirmed through a variety of analytical techniques including melting point, elemental analysis, IR, ^1H NMR, and ^{13}C NMR spectroscopies.[98]

The cationic gold(I)−NHC complexes (**21**−**26**) were evaluated for their *in vitro* antimicrobial activity against a variety of Gram-positive and Gram-negative bacteria and fungal species. The results were compared with those of standard drugs ampicillin and flucytosine (Table 9).

Based on the results from Table 9, gold complexes **21**−**23** showed good and selective activity against both Gram-positive and Gram-negative bacteria with complex **22** showing the most activity against the strains tested, as well as some activity against the fungus *C. albicans*. The 1,3-dimesitylmethylimidazolinium chloride (Mmi) salt exhibited effective and selective antibacterial activity against three Gram-positive (*Staph. epidermidis*, *Staph. aureus*, and *Ec. faecalis*) and one Gram-negative (*P. aeruginosa*) bacterial strains. However, the derived gold(I) complex **24** did not show enhanced activity against any of the strains tested. It is apparent that the functionalization of the nitrogen atoms of the NHC ligands and the complexation with Au(I) at the C2 site influence the antimicrobial activity. Some of the Au(I) complexes presented became completely inactive and some with marked activity. In light of this evidence, it can be deduced that the gold atoms do not necessarily influence the

Downloaded by UNIV MAASTRICHT on August 28, 2009 | http://pubs.acs.org
Publication Date (Web): July 6, 2009 | doi: 10.1021/cr800500u

Table 9. MIC of 21−26[98]

	MIC (μg/mL)[a]						
test compound	*Staph. epidermidis*	*Staph. aureus*	*Ec. faecalis*	*Eb. cloacae*	*P. aeruginosa*	*E. coli*	*C. albicans*
21	800	3.12	800	3.12	1600	800	800
22	6.25	3.12	3.12	1600	3.12	1600	200
23	>1600	>1600	>1600	>1600	>1600	3.12	>1600
24	>1600	200	>1600	100	>1600	200	>1600
25	>1600	50	800	12.5	>1600	1600	1600
26	>1600	50	>1600	800	>1600	400	>1600
Mmi[b]	6.25	3.12	3.12	1600	3.12	400	200
ampicillin	<3.12	>3.12	6.25	<3.12	25	<3.12	
flucytosine							6.25

[a] MIC results are based on 24 h incubation at 37 °C for bacteria and 48 h incubation at 30 °C for fungus. [b] Mmi = 1,3-dimesitylmethylimidazolinium chloride[25]

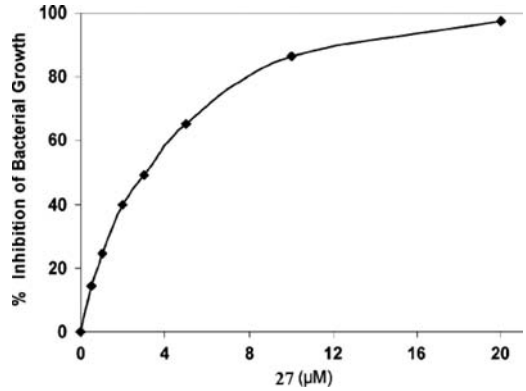

Figure 18. Percent inhibition of *Bac. subtilis* 168 cell proliferation by complex **27**.[73]

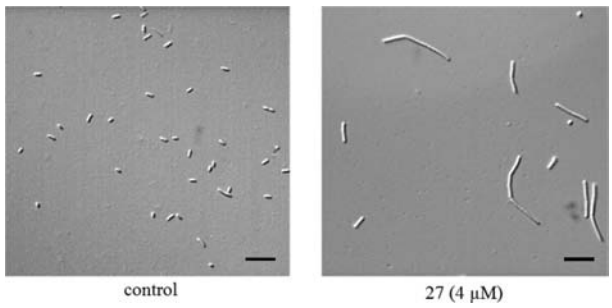

Figure 19. Effects of complex **27** on the morphology of *Bac. subtilis*. Cells were incubated for 4 h in the absence and in the presence of **27**, and the cell morphology was visualized by DIC microscopy. Scale bar represents 10 μm.[73]

Scheme 8. Synthesis of 27[73]

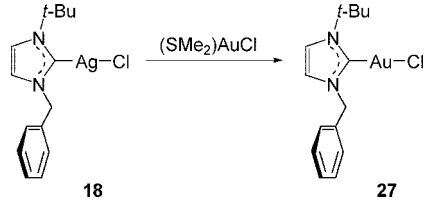

antimicrobial activity but rather it is the type of functional groups bound to the carrier ligands that do.

4.2.2. Synthesis and Antimicrobial Properties of Gold−NHC Complexes Derived from 1-Benzyl-3-tert-butylimidazole

Ghosh and co-workers reported the antimicrobial activity of a gold(I)−NHC complex, [1-benzyl-3-*tert*-butylimidazole-2-ylidene]AuCl (**27**).[73] The complex was synthesized following the carbene-transfer route from the reaction discussed previously of the silver complex **18** with $(SMe_2)AuCl$ (Scheme 8). According to the ^{13}C NMR spectrum, the diagnostic N*C*N−Au resonance appeared at 169.2 ppm, which is observed for analogous Au−NHC complexes.

The antimicrobial efficacy of the gold complex **27** was evaluated against *Bac. subtilis* and *E. coli*. Similarly to the Ag−NHC complex **18**, the Au−NHC complex **27** exhibited antimicrobial activity against *Bac. subtilis* (Figure 18) but had no effect against *E. coli*. Furthermore, the IC_{50} and the MIC values of **27** obtained for the growth of the wild-type *Bac. subtilis* 168 were calculated to be 4 ± 0.8 and 15 ± 2.3 μM, respectively.

In an effort to understand the antimicrobial mechanism of complex **27**, the morphology of the *Bac. subtilis* cells was evaluated after their incubation with 4 μM of **27** for 4 h (Figure 19). The elongation of the *Bac. subtilis* cells by 3.5-fold from 2.2 ± 0.5 μm to 7.3 ± 3.1 μm was observed compared with the control cells grown in the absence of **27**. This elongation suggested that **27** inhibited bacterial proliferation by blocking the cytokinesis step of cell division.[73]

4.3. Synthesis, Antimitochondrial, and Antitumor Properties of Gold−NHC Complexes

Baker and co-workers explored the potential of five compounds of the general formula $[(R_2Im)_2Au]^+$, where Im represents an imidazole, and a series of dinuclear Au(I) complexes as possible antimitochondrial antitumor agents.[99,76] Considering the fact that mitochondrial regulation of apoptosis in tumor cells could be manipulated for therapeutic gain, complexes (**28**−**39**) of different lipophilicities were evaluated for their efficacy in inducing mitochondrial membrane permeabilization (MMP) in isolated rat liver mitochondria. MMP is regulated by the mitochondrial permeability transition pore (MPT), which is considered vital to the mitochondrially induced apoptosis process.

The imidazolium salt precursors were deprotonated *in situ* with lithium hexamethyldisilazide (LiHMDS) in DMF at room temperature followed by the reaction with half the equivalent amounts of $(Me_2S)AuCl$ to yield the corresponding $[(R_2Im)_2Au]^+$ complexes **28**−**32** (Scheme 9).[99] The lipophilicity of the resultant gold−NHC complexes **28**−**32** varied according to the alkyl substituents on the imidazolium salt precursors.

The gold complexes of bridging bidentate NHCs **33**−**39** were synthesized by reacting an equimolar mixture of the desired imidazolium salt with $(Me_2S)AuCl$ in DMF at 100 °C after which a carboxylate salt (sodium acetate, lithium acetate, or lithium butyrate) was added to the solution and allowed to react for an additional 30 min at 120 °C.[100]

Downloaded by UNIV MAASTRICHT on August 28, 2009 | http://pubs.acs.org
Publication Date (Web): July 6, 2009 | doi: 10.1021/cr800500u

Chart 7. Structures of Antimitochondrial Gold(I) Complexes 33−39[76]

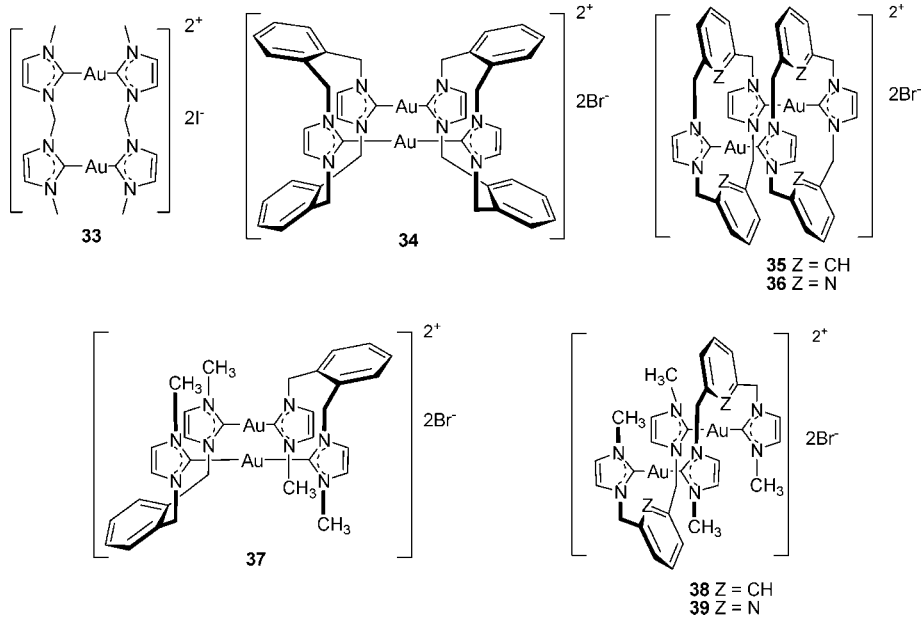

Scheme 9. Synthesis of 28−32[99]

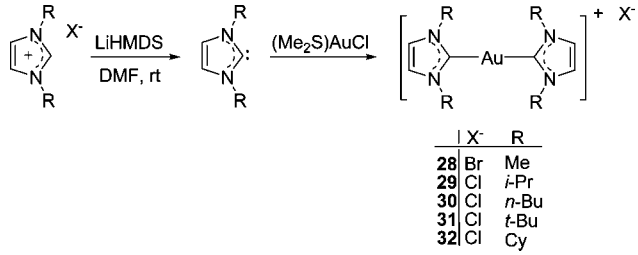

	X-	R
28	Br	Me
29	Cl	*i*-Pr
30	Cl	*n*-Bu
31	Cl	*t*-Bu
32	Cl	Cy

Complexes **33**−**39** shown in Chart 7 precipitated from the reaction mixture.

The ^{1}H and ^{13}C NMR spectral data were in good agreement with the proposed structures. Notably, the ^{1}H NMR spectrum was missing the acidic imidazolium C2−H proton signal and the ^{13}C NMR spectrum showed the appearance of the C2 carbene signal downfield of the C2 carbon signal of the imidazolium salt confirming the formation of the Au−NHC complex. The resulting Au−NHC complexes were further characterized crystallographically. The complexes were synthesized as the halide salt but converted to the hexafluorophosphate salt using KPF_6 in order to obtain crystals suitable for single X-ray diffraction analysis. The structures of complexes **28**·PF_6^- and **30**·PF_6^- are shown in Figure 20.

As mentioned previously, the lipophilicity of complexes **28**−**32** was varied based on the alkyl substituents of the NHC ligands. The results were as expected with complex **28**·Br^- (R = Me) as the least lipophilic and complex **32**·Cl^- (R = Cy) as the most lipophilic. The effect of complexes **28**−**32** on inducing MMP was monitored by measuring the degree of mitochondrial swelling based on the absorbance at 540 nm as a function of time at varying drug concentrations of 1 or 10 μM. At a drug concentration of 1 μM, the time taken to induce mitrochondrial swelling decreased as the degree of lipophilicity increased. Therefore, the least lipophilic complex **28**·Br^- was virtually inactive, whereas the rest of the complexes showed significant activity. At 10 μM however, complexes **29**−**32**·Cl^- showed rapid induction of mitochondrial swelling, and interestingly enough, complex **28**·Br^- showed modest activity at the higher concentration. These results clearly demonstrate the direct dependence of the antimitochondrial activity on lipophilicity.

On the other hand, the dinuclear Au(I)−carbene complexes (**33**−**39**) were found to induce significant mitochondrial swelling at a concentration of 10 μM. Complex **34** induced marked swelling at a submicromolar concentration of 0.5 μM compared with its analogues. A time-dependent assay of Au(I) uptake into the mitochondria of complexes **33**−**39** was performed to establish whether the degree of Au(I) uptake was associated with increased swelling of the mitochondria. However there was no apparent correlation between the two activities indicating that the ability of those complexes to induce MMP does not correlate with their ability to enter the mitochondria. A possible mechanism by which complexes **22**−**39** function could be through the disruption of a certain enzyme or the interaction with components of the MPT.

Baker and co-workers also reported the synthesis of linear Au(I)−NHC complexes as the first NHC analogues for the Au(I) phosphine drug auranofin.[101] The neutral 2,3,4,6-tetra-*O*-acetyl-β-D-glucopyranosyl-1-thiolato complexes [(R_2Im)Au(SR′)] (**40**−**44**) were synthesized by the treatment of [(R_2Im)AuCl] complexes with tetra-*O*-acetyl-β-D-glucopyranose (HSR′) under basic conditions (Scheme 10). The goal was to take advantage of the ease by which N-heterocyclic carbenes can be chemically manipulated to synthesize a range of structurally similar complexes with varying degrees of lipophilicity for biological evaluation. It was stated that according to preliminary biological studies, the antimitochondrial activity of these complexes correlated with their lipophilicity but the results were not shown.

Several recent papers came out addressing the antitumor activity and the underlying cytotoxic mechanisms of Au(I)−NHC complexes.[102−104] In addition, one recent review by Berners-Price addressed recent strategies on targeting the mitochondrial cell death pathway with Au(I)−NHC complexes.[93] Raubenheimer reported the cytotoxicity of a bis-(NHC)Au(I) complex (**45**) carrying an electrophoric, cytotoxic ferrocene moiety.[102] Complex **45** was synthesized through a multistep synthetic procedure (Scheme 11) involving the diazotation and subsquent coupling of ferrocene to

Downloaded by UNIV MAASTRICHT on August 28, 2009 | http://pubs.acs.org
Publication Date (Web): July 6, 2009 | doi: 10.1021/cr800500u

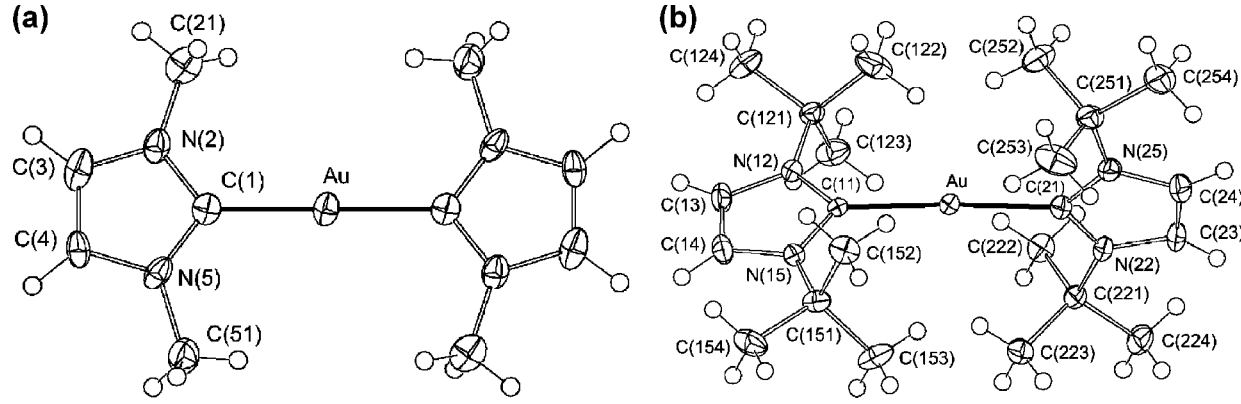

Figure 20. The cationic portion of complexes (a) **28**·PF_6^- and (b) **30**·PF_6^-. Reproduced by permission of The Royal Chemical Society.[99]

Scheme 10. Synthesis of 40−44[101]

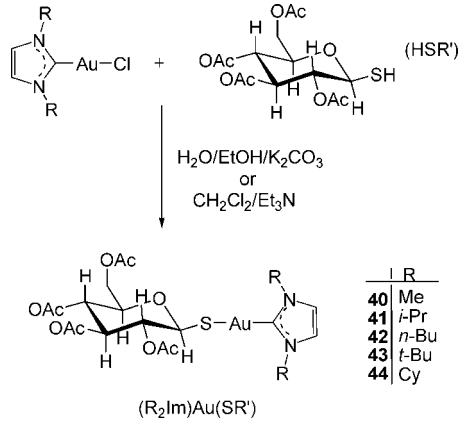

Scheme 11. Synthesis of 45[102]

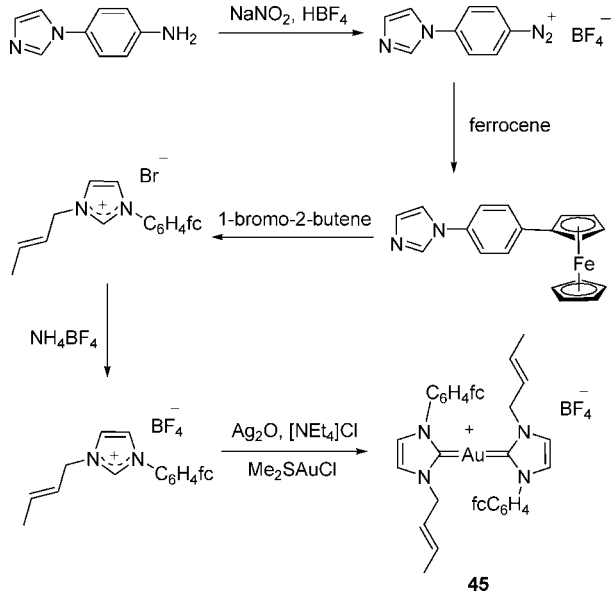

4-(1*H*-imidazole-1-yl)aniline, followed by alkylation with 1-bromo-2-butene in CH_2Cl_2 and anion exchange in acetone. The final bis(NHC)Au(I) ferrocenyl complex was obtained after the reaction with Ag_2O and the subsequent carbene ligand transfer to $(CH_3)_2SAuCl$ in the presence of tetraethylammonium chloride.

The *in vitro* efficacy of complex **45** was determined against human cancer cell lines HeLa (cervical), CoLo 320 DM (colon), Jurkat (leukemia), and MCF-7 (breast) using the MTT assay. Complex **45** was more effective than cisplatin against HeLa and Jurkat cell lines with considerably lower IC_{50} values. Jurkat cells were the most sensitive with an IC_{50} value of 0.253 ± 0.031 μM compared with that of cisplatin (0.783 ± 0.054 μM), while the CoLo cells were the least sensitive with an IC_{50} value of 1.007 ± 0.081 μM compared with that of cisplatin (0.407 ± 0.043 μM). This was an indication that complex **45** is selective in its performance against certain types of cancer. The effect of complex **45** on normal human lymphocytes was also investigated. It was determined that normal cells were less sensitive to complex **45**, which further highlights its selectivity to cancer cells.[102]

Filipovska and co-workers investigated the antitumor activity and cytotoxic mechanism of a previously discussed Au(I)−NHC complex **29** against two liver progenitor cell (LPC) lines, one nontumorigenic [p53-immortalized liver (PIL) 4] and the other tumorigenic (PIL2).[103] The goal was to exploit the increase in mitochondrial membrane potential ($\Delta\Psi_m$) in cancer cells for the development of mitochondria-targeted chemotherapeutics that selectively target tumor cells. This can be achieved by the use of delocalized lipophilic cations (DLCs), which can pass easily through the lipid bilayer as a consequence of their positive charge and preferentially accumulate in the mitochondria of tumorigenic cells because of the large $\Delta\Psi_m$ thereby directly exerting their destructive effect.[93] The lipophilic, cationic Au(I)−NHC complex **29** exhibited notable selective toxicity for the tumorigenic PIL2, with elevated $\Delta\Psi_m$ compared with nontumorigenic PIL4 cells.[103]

Complex **29** was shown to accumulate in the mitochondria of PIL2 cells by measuring the mitochondrial gold concentration using ICP-MS. The mitochondrial concentration of gold increased with increasing concentrations of complex **29** given. When PIL2 cells were treated with 4 μM of complex **29**, >50% cell growth inhibition was observed and >80% of the gold content was found accumulated within the mitochondria. The distribution of the gold was found shifted to the cytoplasm with the dissipation of $\Delta\Psi_m$ with the uncoupler carbonyl cyanide 4-(trifluoromethoxy)phenylhydrazone. This further proves that the cationic gold(I) complex accumulates in the mitochondria of cells driven by the $\Delta\Psi_m$.

Furthermore, to demonstrate the selective inhibition of PIL cell growth by complex **29**, PIL2 and PIL4 cells were treated with Au(I) complex over 72 h, and it was shown that the growth of PIL2 cells was inhibited by 50% after a 48 h incubation and >80% of total ATP was lost after 72 h. In contrast, the growth and total ATP in the PIL4 cells were not affected.[103] These data substantiate the selective toxicity of complex **29** toward the tumorigenic PIL2 cells compared

Downloaded by UNIV MAASTRICHT on August 28, 2009 | http://pubs.acs.org
Publication Date (Web): July 6, 2009 | doi: 10.1021/cr800500u

Scheme 12. Synthetic Routes to Ruthenium(II)−Carbene Complexes[120,121]

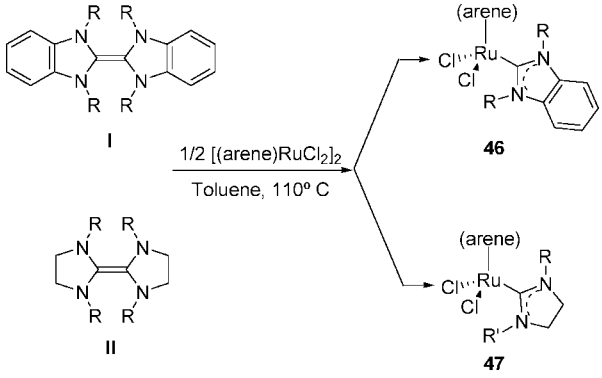

	arene	R	R'
46a	*p*-$MeC_6H_4Pr^i$	Me	-
46b	*p*-$MeC_6H_4Pr^i$	Et	-
46c	$C_6H_3Me_3$	Me	-
46d	$C_6H_3Me_3$	Et	-
46e	C_6Me_6	Me	-
46f	C_6Me_6	Et	-
47a	*p*-$MeC_6H_4Pr^i$	Me	CH_2CH_2OMe
47b	*p*-$MeC_6H_4Pr^i$	CH_2CH_2OMe	CH_2CH_2OMe
47c	*p*-$MeC_6H_4Pr^i$	*p*-$CH_2C_6H_4OMe$	*p*-$CH_2C_6H_4OMe$
47d	*p*-$MeC_6H_4Pr^i$	*p*-$CH_2C_6H_4N(Me)_2$	*p*-$CH_2C_6H_4N(Me)_2$
47e	*p*-$MeC_6H_4Pr^i$	*p*-$CH_2C_6H_4N(Me)_2$·HCl	*p*-$CH_2C_6H_4N(Me)_2$·HCl
47f	C_6Me_6	Me	CH_2CH_2OMe
47g	C_6Me_6	CH_2CH_2OMe	CH_2CH_2OMe
47h	C_6Me_6	*p*-$CH_2C_6H_4OMe$	*p*-$CH_2C_6H_4OMe$
47i	C_6Me_6	*p*-$CH_2C_6H_4N(Me)_2$	*p*-$CH_2C_6H_4N(Me)_2$
47j	C_6Me_6	*p*-$CH_2C_6H_4N(Me)_2$·HCl	*p*-$CH_2C_6H_4N(Me)_2$·HCl

Chart 8. Structures of Ru(II) Complexes 48a and 48b[121]

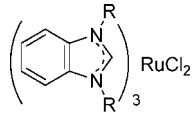

48a R = Me
48b R = Et

with the nontumorigenic PIL4 cells. Complex **29** was also shown to selectively induce cell death in the tumorigenic PIL2 cells through a mitochondrial apoptotic pathway.[103] This was demonstrated by following a two-step process. The amount of caspase-3 activation, which is used as a marker for apoptosis, was measured. A marked increase in caspase-3 activation was observed in PIL2 cells after 12 h of incubation with complex **29**, whereas no caspase-3 activation was observed for PIL4. This result confirms the induction of cell death by activating the apoptotic pathway. The next step was to confirm that complex **29** induced apoptosis via the mitochondria, which was demonstrated by the incubation of the PIL2 cells with complex **29** and noting a 3-fold increase in caspase-9 activity.[103]

Next, Filipovska and co-workers aimed to rationally design an antitumor agent that combined selective mitochondrial targeting along with selective thioredoxin reductase (TrxR) inhibition.[104] Increased activity of TrxR was found to correlate with the acceleration of tumor growth, and therefore the inhibition of this system has become an important drug target. Au(I) complexes are known to be potent inhibitors of mammalian TrxR, where their activity is exerted through Au(I) binding to the C-terminal redox active -Cys-Sec- center of TrxR.[93,94] The group investigated the effects of complex **29** against cell growth of two highly tumorigenic breast cell lines, MDA-MB-231 and MDA-MB-468, as well as normal human mammary epithelial cells (HMEC). Complex **29** was chosen over two other Au(I)−NHC complexes due to its intermediate lipophilicity (log $P = -0.83$) and thus superior cytotoxic potency and selectivity.[99,104] Complex **29** exhibited the same selective mitochondrial targeting characteristics on MDA-MB-231, MDA-MB-468, and HMEC as those observed against tumorigenic PIL2 and nontumorigenic PIL4 cells. Additionally, MDA-MB-231 cells were treated with increasing concentrations of complex **29** for 6 h. TrxR activity was inhibited by nearly 50% with a 5 μM concentration of complex **29**. These data underscore the successful attempt at the design of mitochondria-targeted chemotherapeutics that are selectively toxic to cancer cells as well as allow targeting and thus selective inhibition of mitochondrial selenoproteins, such as TrxR.[104]

5. Ruthenium and Rhodium

5.1. Medical Uses of Ruthenium and Rhodium Compounds

Ruthenium is mostly known for its use in the development of new antitumor agents. The first Ru(III) complexes explored for their antitumor activity were chloro-ammino-Ru(III) complexes, such as *cis*-$[RuCl_2(NH_3)_4]Cl$, *trans*-$[RuCl_4(Im)_2](HIm)$, and *fac*-$[RuCl_3(NH_3)_3]$. While this class of Ru(III) complexes was very active against primary tumors, *fac*-$[RuCl_3(NH_3)_3]$ was determined unsuitable as an antitumor agent due to its poor water solubility.[105,106] *trans*-$[RuCl_4(Im)_2](HIm)$, known as the Keppler-type complex, exhibited better tumor inhibition than cyclophosphamide, cisplatin, and 5-fluorouracil when examined against P388 leukemia and B16 melanoma, as well as against platinum-resistant colorectal tumors. Results show that a single dose of 72 mg/kg improved the life-span of animals inoculated with P388 leukemia and multiple doses of 8 mg/kg reduced tumor weights in animals inoculated with B16 melanoma in comparison with the control groups.[107]

A class of chloro-dimethylsulfoxide−Ru(II) complexes with significantly lowered toxicity, namely, *cis*- and *trans*-$[RuCl_2(dmso)_4]$, was also investigated. The coordinating dimethylsulfoxide ligands enhanced the selectivity of the ruthenium complexes for solid tumor metastases but lowered their activity compared with cisplatin. The *cis*-$[RuCl_2(dmso)_4]$ isomer exhibited less activity against Ehrlich ascites carcinoma and L1210 leukemia than cisplatin but was significantly less toxic.[108]

Among the most promising Ru-based antitumor agents is the complex (HIm) *trans*-$[RuCl_4(dmso\text{-}S)(Im)]$ (Im = imidazole, dmso = dimethylsulfoxide), known as NAMI-A, which demonstrated excellent antimetastatic activity against solid tumors. It interfered with the growth of malignant lung metastatic tumors such as Lewis lung carcinoma (LLC), MCa mammary carcinoma, and TS/A adenocarcinoma. NAMI-A was the first ruthenium complex to enter and complete phase I clinical trials.[105,106] A number of other ruthenium complexes bearing various ligands such as arenes,[109] 2-phenylazopyridine (azypy),[110] and 2,2′:6′,2″-terpyridine (terpy)[111] among others have been developed and evaluated for their antitumor activity.

Rhodium complexes were also investigated for their antitumor activity. The majority of these tested complexes were either active but very toxic or not as effective as cisplatin. In particular, a class of dirhodium complexes $[\mu\text{-}(RCO_2)_4Rh_2(H_2O)_2]$ (R = Me, Et, Pr), exhibited good *in vivo* antitumor activity against several tumor types such as Ehrlich ascites, sarcoma 180, and P388 lymphocytic leuke-

Downloaded by UNIV MAASTRICHT on August 28, 2009 | http://pubs.acs.org
Publication Date (Web): July 6, 2009 | doi: 10.1021/cr800500u

Table 10. MIC of Ru(II) Complexes 46−48[120,121]

	MIC (μg/mL)[a]					
compound	*Ec. faecalis*	*Staph. aureus*	*E. coli*	*P. aeruginosa*	*C. albicans*	*C. tropicalis*
46a	100	100	>1000	>1000		
46b	800	1000	800	1000		
46c	200	50	>1000	>1000		
46d	200	200	1000	1000		
46e	50	25	1000	1000		
46f	100	100	1000	1000		
47a	>800	>800	>800	>800	>800	>800
47b	800	>800	>800	>800	>800	>800
47c	100	100	>800	>800	800	200
47d	100	100	>800	>800	100	100
47e	100	25	>800	>800	100	100
47f	>800	>800	>800	>800	400	>800
47g	200	>800	>800	>800	>800	>800
47h	50	50	>800	>800	200	100
47i	50	50	>800	>800	200	200
47j	100	50	>800	>800	200	200
48a	6.25	6.25	1000	1000		
48b	25	12.5	800	800		
ampicillin	0.78	0.39	3.12	<75		

[a] MIC results are based on 16−20 h incubation at 35 °C for bacteria and 48 h incubation at 35 °C for fungi.

Downloaded by UNIV MAASTRICHT on August 28, 2009 | http://pubs.acs.org
Publication Date (Web): July 6, 2009 | doi: 10.1021/cr800500u

Scheme 13. Synthetic Routes to Rhodium(I)−Carbene Complexes

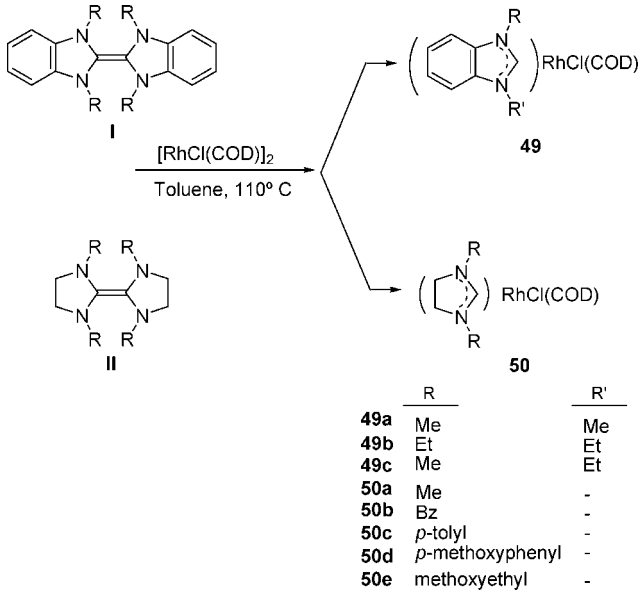

Chart 9. Structures of Rh(I) Complexes 51a, 51b, and 52

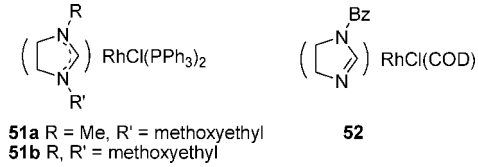

Table 11. MIC of Rh(I) Complexes 49−52[121]

	MIC (μg/mL)[a]			
compound	*Ec. faecalis*	*Staph. aureus*	*E. coli*	*P. aeruginosa*
49a	5	5	>1000	>1000
49b	25	25	200	400
49c	5	5	1000	1000
50a	400	50	800	1000
50b	50	50	>1000	>1000
50c	200	200	200	200
50d	50	25	1000	>1000
50e	25	25	>1000	>1000
51a	25	25	>1000	>1000
51b	100	25	1000	1000
52	400	400	400	400
ampicillin	0.78	0.39	3.12	<75

[a] MIC results are based on 16−20 h incubation at 35 °C.

mia; however severe toxic side effects prevented their advancement.[106,112] Fine-tuning of characteristic features, lipophilicity, charge, solubility, lability of bridging groups, etc., has led to the design of additional dirhodium complexes in order to reach a compromising median between antitumor activity and toxic side effects.[112]

Other monomeric, square-planar Rh(I) complexes such as [(COD)(PMI)Rh]Cl (PMI = 2-pyridinalmethylimine, COD = cyclooctadiene) seemed active against metastatic tumors including MCa mammary carcinoma and Lewis lung carcinoma. Furthermore, Rh(III) complexes analogous to those of ruthenium(III) complexes described above were either inactive or possessed modest levels of activity when tested against primary or metastatic MCa mammary tumors in the lung.[106,113]

For more comprehensive and recent reviews on the medicinal developments of rhodium and ruthenium metal complexes, the reader is directed to the recent contributions by Liu,[114] Sadler,[115] and Reedijk.[116]

5.1.1. Mechanisms of Ruthenium and Rhodium Activity

Ruthenium-based complexes are thought to act through three major mechanisms, which potentially explain their selectivity to solid and metastatic tumors. Experiments with $RuCl_3$ and calf-thymus DNA conducted by Sideris and co-workers found that there was little interaction between the two reagents perhaps through cross-linking.[117] To further verify this theory, Reedijk and co-workers showed that *mer*-[Ru(terpy)Cl_3] bound to guanine derivatives in a *trans* configuration and formed DNA interstrand cross-links.[111] Therefore, multichloro ruthenium(III) complexes appear to favor interstrand cross-links with guanine N7 sites. This mechanism differs from cisplatin, which forms intrastrand cross-links.

Moreover, ruthenium has the ability to mimic iron due to their chemical similarity and bind to transferrin.[106,118] Rapidly dividing tumor cells have a higher requirement for iron in comparison to normal cells and therefore have an increased

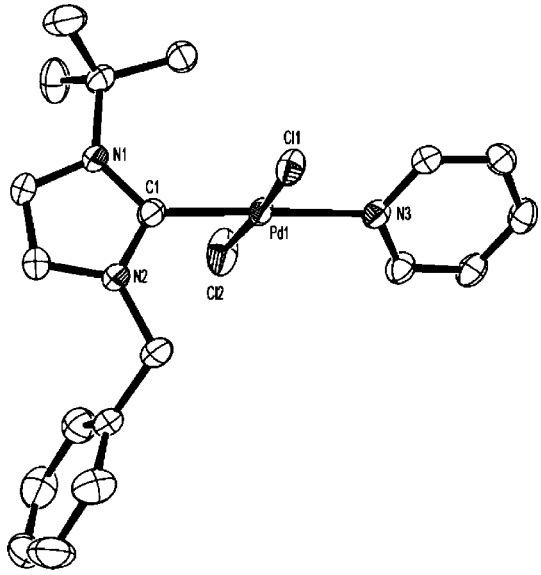

Figure 21. Molecular structure of **56**.[73]

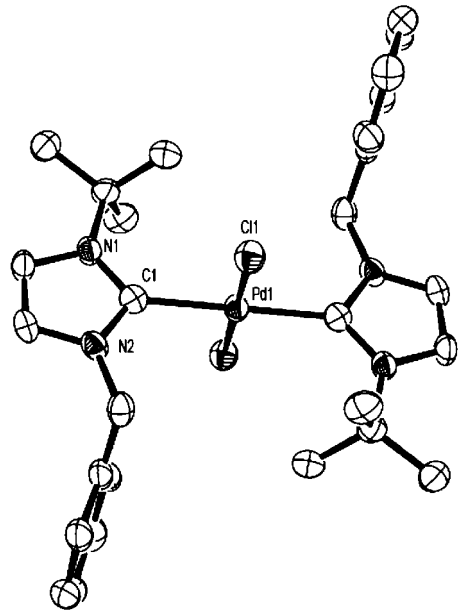

Figure 22. Molecular structure of **57**.[73]

Chart 10. Structures of Pd Complexes 53−55

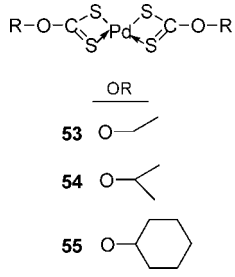

number of transferrin receptors on their cell surface. Once ruthenium reaches the cell surface, apotransferrin can then act as a selective carrier of Ru drugs into the tumor cells. This characteristic is thought to contribute to ruthenium's low toxicity.

Rapidly growing tumors are also known to possess low oxygen content and lower pH than normal cells. This type of environment favors the binding of Ru(II) complexes, which are more active *in vivo* than Ru(III). Therefore, Ru(III) complexes are thought to serve as prodrugs and readily undergo reduction to Ru(II) by glutathione and other redox proteins present *in vivo*.[106,118] This suggested mechanism is known as "activation by reduction". Work done by Clarke demonstrating the increased inhibition of growth in HeLa cells with added transferrin and lower partial pressures of oxygen (P_{O_2}) further confirmed the above suggested mechanisms.[119]

The *in vivo* mechanism of rhodium compounds has not been investigated thoroughly. However, structural studies with dirhodium complexes suggested their analogy to cisplatin in binding to adjacent guanines on DNA and forming intrastrand cross-links.[112] Additionally, rhodium(III) complexes are structurally similar to ruthenium(III) complexes and yet their activation by reduction to rhodium(II) is not likely. This is perhaps due to their enhanced inertness in comparison to their ruthenium analogues, which explains their reduced antitumor activity.[113]

Scheme 14. Synthetic Routes to Palladium(II)−Carbene Complexes[73]

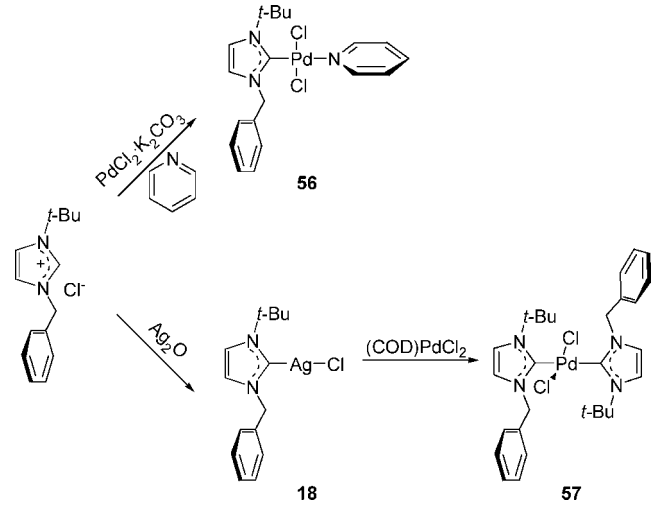

Table 12. Half-Maximal Inhibitory Concentration (IC_{50}) of 53−55[123]

	IC_{50} Calu-6		IC_{50} MCF7	
compound	pH 6.8	pH 7.4	pH 6.8	pH 7.4
cisplatin	26.04	27.21	122.50	207.66
53	0.32	1.50	1.17	5.31
54	0.10	0.46	0.45	2.17
55	0.47	1.02	0.63	2.43

Table 13. Percent Inhibition of HeLa Cell Proliferation by 56 and 57[73]

	inhibition, %	
concentration (μM)	**56**	**57**
1	7 ± 3	7 ± 3
5	23 ± 4	57 ± 3
10	35 ± 3	85 ± 2

Table 14. Half-Maximal Inhibitory Concentrations (IC_{50}) of 56c Compared with Cisplatin Using the SRB Assay[73]

	IC_{50} (μM)		
compound	HeLa	HCT 116	MCF-7
cisplatin	8 ± 1	16 ± 3	15 ± 2
57	4 ± 0.2	0.8 ± 0.05	1 ± 3

Downloaded by UNIV MAASTRICHT on August 28, 2009 | http://pubs.acs.org
Publication Date (Web): July 6, 2009 | doi: 10.1021/cr800500u

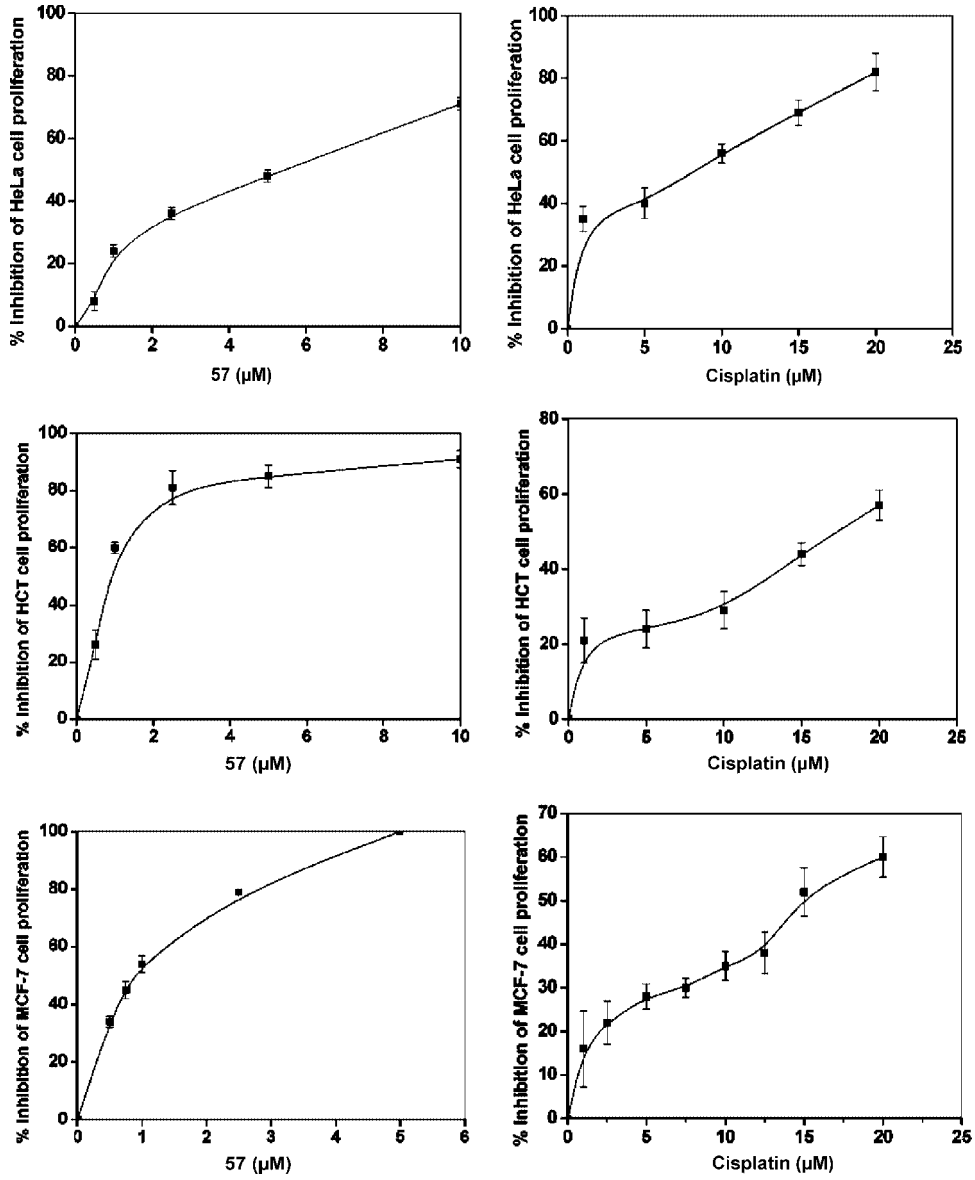

Figure 23. Inhibition of HeLa, HCT 116, and MCF-7 cell proliferation by **57** and cisplatin, measured using the SRB assay.[73]

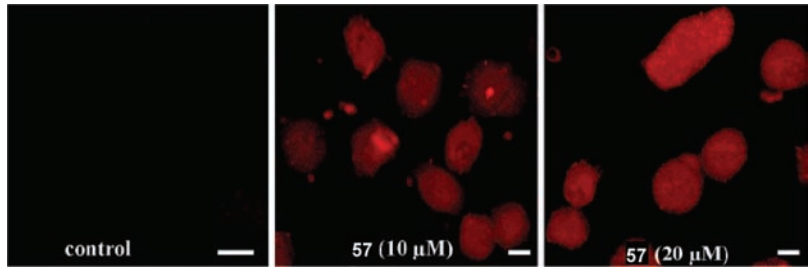

Figure 24. Immunofluorescence analysis of HeLa cells arrested at the G2/M phase of the cell cycle after treatment with **57** at 10 and 20 μM. The cells were stained with cyclin B1 antibody. The figure demonstrates the overexpression of cyclin B1 in the treated cells compared with the control.[73] Scale bar represents 10 μM.

5.2. Synthesis and Antimicrobial Properties of Rhodium− and Ruthenium−NHC Complexes

Although the antitumor activity and mechanism of action for both ruthenium and rhodium metals has been discussed above, no accounts of antitumor activity of ruthenium and rhodium NHCs were found in the literature. Based on their antitumor efficacy, especially that of Ru, the exploration of the antitumor potential of Ru NHCs is highly recommended. Having said that, this section will focus on the role of the two metal NHCs as antimicrobial agents.

Cetinkaya and co-workers were the first to investigate the *in vitro* antimicrobial activity of Rh(I)− and Ru(II)−carbene complexes. The ruthenium complexes (**46**, **47**) were synthesized by treating the electron-rich olefins (**I** or **II**) with half the equivalents of the appropriate $[(arene)RuCl_2]_2$ in refluxing toluene (Scheme 12).[120,121] Other similar ruthenium com-

Downloaded by UNIV MAASTRICHT on August 28, 2009 | http://pubs.acs.org
Publication Date (Web): July 6, 2009 | doi: 10.1021/cr800500u

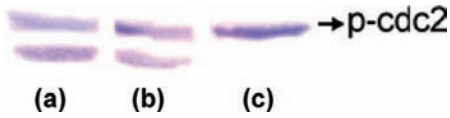

Figure 25. Western blot analysis of the cell lysate treated with (a) vehicle, (b) 10 μM **57**, and (c) 20 μM **57**. Phospho-cdc2 antibody (p-cdc2), which is specific to the G2 phase, was used. Phosphorylation was particularly increased in 20 μM **57**-treated cells. The figure indicates the inactivation of cdc2 by phosphorylation, which arrested the cells at the G2 phase. The top band is the phosphorylated form and the botton band is the unphosphorylated form of cdc2.[73]

plexes, **48a** and **48b**, were synthesized following the same general procedure (Chart 8).[121] All of the complexes were analyzed using ^{1}H NMR and FT-IR spectroscopies and melting points.

The antimicrobial activity of the ruthenium complexes (**46**−**48**) was evaluated against *Ec. faecalis*, *Staph. aureus*, *E. coli*, and *P. aeruginosa*.[120,121] In addition, the antifungal activity of complexes **47a**−**j** against *C. albicans* and *C. tropicalis* was investigated.[120] Ampicillin was used as a reference compound. The results are summarized in Table 10.

As observed from Table 10, none of the ruthenium complexes tested is as effective at killing bacteria as the reference compound ampicillin. Complex **48a** however came closest with MIC values of 6.25 μg/mL againt both *Ec. faecalis* and *Staph. aureus*, followed by **48b** with MIC values of 25 and 12.5 μg/mL againt these bacteria, respectively. Complexes **46a** and **46c**−**f** showed some activity with MIC values ranging between 25 to 100 μg/mL, whereas **46b** exhibited no activity against any of the bacterial organisms tested. Complexes **47a**−**j** also exhibited limited to no activity. In particular, complexes **47a**, **47b**, and **47f** were completely inactive with antibacterial MIC values of 800 or more. More significant activity against Gram-positive bacteria and fungi was observed with complexes **47c**, **47d**, **47e**, **47g**, **47h**, **47i**, and **47j**. None of the Ru(II) complexes mentioned exhibited any activity against the Gram-negative bacteria *E. coli*.

It is worth noting that the investigators looked into the antimicrobial efficacy of other ruthenium(II) complexes bearing other nitrogen-donating ligands; however the carbene derivatives showed more pronounced activity. Interestingly, more potent activity within this group of compounds was observed with those bearing more lipophilic substituents compared with their analogues. Lipophilic side chains evidently enhance the capability of antimicrobial agents to cross the bacterial cellular membrane, thus providing an important insight for the future design of efficacious antimicrobials that is consistent with previous studies.[26]

As mentioned previously, the antimicrobial efficacy of Rh(I) carbene complexes was also evaluated. The synthetic procedure followed that of the Ru(II) carbene complexes where the electron rich olefin **II** and its benzimidazole derivative **I** were reacted with the chloro-bridged dimer $[RhCl(COD)]_2$ in refluxing toluene to yield complexes (**49**−**50**) (Scheme 13).[121] Complex (**51**) however was made by utilizing a different Rh(I) compound with two triphenylphosphine ligands and complex (**52**) was synthesized by the treatment of 1-benzyl-2-imidazoline with $[RhCl(COD)]_2$ (Chart 9).[121] All of the reactions described were carried out under oxygen-free conditions. The purity of the complexes was analyzed with the aid of ^{1}H NMR and FT-IR spectroscopies and melting point techniques.

The antimicrobial efficacy of the rhodium(I) complexes **49**−**52** was investigated against the bacterial strains *Ec. faecalis*, *Staph. aureus*, *E. coli*, and *P. aeruginosa*.[121] Ampicillin was used as a reference compound, and the MIC values of the complexes along with the control compound are reported in Table 11.

Based on the results in Table 11, more Rh(I) complexes have shown greater antimicrobial activity than structurally similar Ru(II) complexes. Particularly, complexes **49a**−**c**, **50b**, **50d**, **50e**, and **51a** were mostly effective against the Gram-positive bacteria *Ec. faecalis* and *Staph. aureus* with MIC values ranging between 5−50 μg/mL. None of the complexes shown in Table 11 seemed active against the Gram-negative bacteria *E. coli* and *P. aeruginosa*. The enhanced activity of the Ru(II) and Rh(I) complexes against the Gram-positive bacteria and their diminished activity against the Gram-negative bacteria could be related to the difference in their bacterial cell wall structure. Gram-negative bacteria have an additional outer membrane protecting their thin peptidoglycan layer, which could contribute to the reduced activity against them due to limited penetration of the metal complexes through the membrane.

6. Palladium

6.1. Medicinal Uses of Palladium Compounds

Palladium, being structurally similar to platinum, has been explored as a potential alternative to treat several types of cancers unresponsive to current chemotherapeutic treatments. Several different palladium complexes were investigated for their antiproliferative activity against tumor cells.[122−125]

Amtmann and co-workers investigated the antitumor activity of Pd−xanthate complexes on two human cancer cell lines, Calu-6 (lung adenocarcinoma) and MCF-7 (mamma carcinoma).[125] The palladium complexes **53**−**55**, shown in Chart 10, exhibited superior activity compared with other metal−xanthate complexes tested.

The IC_{50} values ranged between 0.1 and 0.47 μM in Calu-6 and between 0.45 and 1.17 μM in MCF-7 cells (Table 12). Further studies on the differential activity of complexes

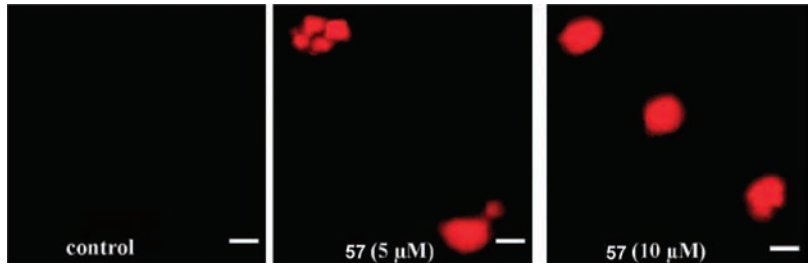

Figure 26. HeLa cells incubated with 5 and 10 μM of **57** for 24 h and then visualized with propidium iodide staining. Dead or dying cells are stained red due to the penetration of propidium iodide through the cell membrane, whereas the control cells lack the stain indicating their viability.[73] Scale bar represents 10 μM.

Downloaded by UNIV MAASTRICHT on August 28, 2009 | http://pubs.acs.org
Publication Date (Web): July 6, 2009 | doi: 10.1021/cr800500u

(**53**−**55**) on cell lines Calu-6 and MCF-7 at pH 6.8 and 7.4 (pH of normal cells) proved the enhanced cytotoxicity of the Pd complexes under slightly acidic conditions, namely, pH 6.8. This is of interest since this is a common occurrence in solid tumors due to the production of lactic acid.

Gonzalez conducted DNA-binding studies of two Pd(II) complexes vs cisplatin. They concluded that their Pd(II) complexes interact with DNA at a faster rate than cisplatin and produce the same amount of DNA destabilization at lower concentrations.[126] Furthermore, a comparative study evaluating the biological activity of a *trans*-Pd(II) complex bearing a pyrazole containing ligand confirmed its enhanced cytotoxicity against two human leukemia cell lines, HL-60 and NALM-6, compared with its *cis*-Pt(II) counterpart with the same ligand system.[127] Several other palladium(II) complexes with nitrogen-containing ligands, such as Pd−pyridine[126−129] and Pd−amine[130−134] complexes have been shown to possess antitumor activity.

For more comprehensive and recent reviews on the medicinal developments of palladium metal complexes and their use as chemotherapeutic agents, the reader is directed to the recent contributions by Abdalla[135] and Caires.[136]

Downloaded by UNIV MAASTRICHT on August 28, 2009 | http://pubs.acs.org
Publication Date (Web): July 6, 2009 | doi: 10.1021/cr800500u

6.2. Synthesis and Antitumor Properties of Palladium−NHC Complexes

Although the biological activity of Pd-based drugs bearing a variety of ancillary ligands has been under intense investigation, only one report of Pd−NHC complexes with anticancer activity is found in recent literature. Ghosh took the initiative of exploring the cytotoxic capacity of two Pd complexes, (NHC)Pd(pyridine)Cl_2 (**56**) and $(NHC)_2PdCl_2$ (**57**) against three human tumor cell lines *in vitro*.[73]

Complex **56** was synthesized by the direct reaction of 1-benzyl-3-*tert*-butylimidazolium chloride with $PdCl_2$ in pyridine. Complex **57** was obtained by a transmetalation route, employing the previously discussed silver complex **18** and (COD)$PdCl_2$ (Scheme 14). Both complexes were evaluated using ^{13}C NMR, which confirmed the presence of the N*C*N-Pd metal bond by the appearance of resonances at 151.4 ppm and 166.9 ppm for complexes **56** and **57**, respectively. These shifts fall within the range (δ 175−145 ppm) of other Pd−NHC metal complexes.[137]

The formation of the two metal complexes was further proved by X-ray diffraction studies (Figures 21 and 22). The Pd−metal centers of both complexes were shown to exist in square-planer geometries and the substituents on the N-1 and N-3 positions of both NHC ligands are oriented *trans* with respect to each other.

The Pd−NHC complexes **56** and **57** were evaluated for their antitumor activity in terms of the percent inhibition of HeLa cell proliferation, and the results are summarized in Table 13. Complex **57**, the more cytotoxic of the two Pd complexes, was compared with cisplatin (Table 14).

The results revealed that **57** inhibited the growth of HeLa (cervical cancer), MCF-7 (breast cancer), and HCT 116 (colon adenocarcinoma) cells rather potently in a concentration-dependent manner (Table 14, Figure 23). The cell proliferation was measured using the sulforhodamine B (SRB) assay, in which tumor cells are incubated with different concentrations of the test compound for one cell cycle.[138] Figure 23 shows that **57** has a stronger inhibition effect compared with cisplatin under similar conditions.

6.2.1. Mechanism of Palladium−NHC Complex Activity

The properties of the Pd(II) complex **57** are of interest due to its enhanced *in vitro* activity against the tumor cell lines tested compared with cisplatin, the most widely used chemotherapeutic agent. To further understand the mechanistic pathway employed by **57**, HeLa cells were incubated with different concentrations of **57** for 24 h. The goal was to study the effects of **57** on the cell cycle because cisplatin and other analogous Pt(II) complexes are known to induce DNA damage by arresting the cells in the G2/M phase of the cell cycle and thus hinder their growth.[139,140] Two proteins, cdc2 (also known as cdk1) and cyclin B1, are known to regulate the progression of cells from the G2 to the M phase. Cdc2 is a member of a family of kinases called cyclin-dependent protein kinases (CDKs), whose role is to mediate stages of mitosis. Cdc regulates entry into mitosis. It is phosphorylated on Thr14 and Tyr15 residues prior to its association with the protein cyclin B1 to form an inactive complex. This complex is inactive because the phosphorylation of the 14 and 15 residues blocks the ATP binding site of the kinase. During transition from the G2 to the M phase, the kinase is activated by dephosphorylating Thr14 and Tyr15 residues.

The HeLa cells were stained with antibodies against cyclin B1 and phospho-cdc2 in order to evaluate the ability of complex **57** to regulate these two proteins and in turn induce cell cycle arrest. The results of the study revealed that **57** caused overexpression of cyclin B1 in the cells (Figure 24), which suggests G2/M arrest and induction of apoptosis.[141] This only reveals that **57** caused the arrest of the HeLa cells in the G2/M phase because cyclin B1 is specific to the G2/M phase in general. The phospho-cdc2 antibody is particularly specific to the G2 phase, and it revealed the increase in cdc2 phophorylation, thus inactivation of cdc2, after treatment with 20 μM **57**, subsequently proving that **57**-treated cells are arrested in the G2 phase (Figure 25).

Additional studies revealed the ensuing apoptotic cell death following G2 arrest. Live and dead cells treated with **57** at different concentrations (0, 5, and 10 μM) for 24 h were visualized using propidium iodide staining (Figure 26). Propidium iodide is excluded by viable cells but can penetrate the cell membrane of dying or already dead cells. Cells treated with **57** stained positive for propidium iodide after 24 h, which indicates that the cells were either in late apoptosis or had undergone necrosis. The control cells lacked propidium iodide staining, indicating that they were still viable.

7. Conclusion

It is evident from the chemistry highlighted in this section that metal-based pharmaceuticals are highly sought-after for their antitumor or antimicrobial properties. There is relatively little information known about how metal-based drugs function and therefore many studies have been aimed at exploring the mechanistic pathways employed by these drugs. One interesting trend observed among some metals such as ruthenium and silver is that each one utilizes multiple biological mechanisms and can work by a variety of different routes. This multifaceted approach could perhaps contribute to their enhanced activity compared with other metals such as rhodium and low occurrence of resistance toward them compared with platinum.

The pharmaceutical application of NHCs and their metal complexes is a relatively new area that has been gaining interest and has been explored by only a handful of researchers. NHCs are a versatile class of ligands that can be manipulated easily. They possess the ability to bind to both hard and soft metals and can be readily functionalized, which is a promising aspect in terms of designing suitably targeted pharmaceuticals. The lipophilicity of NHCs and most of their metal complexes seems to be important in contributing to both their antimicrobial and antitumor effects as in the case of some imidazolium salts, gold(I)−NHCs, and ruthenium(II)−NHCs. Silver NHCs seem to be the most efficacious in terms of their antimicrobial activity and low toxicity compared with other antimicrobial metal−NHCs including Ru(II) and Rh(I).

8. Acknowledgments

Author K.M.H. would like to thank Dr. Douglas A. Medvetz for helpful discussions in the preparations of this manuscript. Also, the authors would like to thank Dr. Michael J. Taschner, Dr. Daniel Ely, and Dr. Peter L. Rinaldi for useful discussions in the preparation of this review. The authors would like to thank the National Institute of Allergies and Infectious Diseases (Grant 1 R01 A106785601) for support during the preparation of this manuscript.

9. Note Added after ASAP Publication

Co-author Claire A. Tessier was added to the manuscript and her name was removed from the Acknowledgments section. This paper originally posted to the web on July 6, 2009, and reposted on July 24, 2009.

10. References

(1) Öfele, K. *J. Organomet. Chem.* **1968**, *12*, P42–P43.
(2) Wanzlick, H.-W.; Schönberr, H.-J. *Angew. Chem., Int. Ed. Engl.* **1968**, *7*, 141–142.
(3) Arduengo, A. J., III; Harlow, R. L.; Kline, M. *J. Am. Chem. Soc.* **1991**, *113*, 361–363.
(4) Herrmann, W. A. *Angew. Chem., Int. Ed.* **2002**, *41*, 1290–1309.
(5) Bourissou, D.; Guerret, O.; Gabbai, F. P.; Bertrand, G. *Chem. Rev.* **2000**, *100*, 39–91.
(6) Herrmann, W. A.; Kocher, C. *Angew. Chem., Int. Ed. Engl.* **1997**, *36*, 2162–2187.
(7) Herrmann, W. A.; Goossen, L. J.; Spiegler, M. *Organometallics* **1998**, *17*, 2162–2168.
(8) McGuinness, D. S.; Cavell, K. J.; Skelton, B. W.; White, A. H. *Organometallics* **1999**, *18*, 1596–1605.
(9) Hu, X.; Castro-Rodriguez, I.; Olsen, K.; Meyer, K. *Organometallics* **2004**, *23*, 755–764.
(10) Nemcsok, D.; Wichmann, K.; Frenking, G. *Organometallics* **2004**, *23*, 3640–3646.
(11) Samantaray, M. K.; Roy, D.; Patra, A.; Stephen, R.; Saikh, M.; Sunoj, R. B.; Ghosh, P. *J. Organomet. Chem.* **2006**, *691*, 3797–3805.
(12) Samantaray, M. K.; Katiyar, V.; Roy, D.; Pang, K.; Nanavati, H.; Stephen, R.; Sunoj, R. B.; Ghosh, P. *Eur. J. Inorg. Chem.* **2006**, 2975–2984.
(13) Ray, L.; Shaikh, M. M.; Ghosh, P. *Dalton Trans.* **2007**, 4546–4555.
(14) Ray, L.; Barman, S.; Shaikh, M. M.; Ghosh, P. *Chem.—Eur. J.* **2008**, 6646–6655.
(15) Ray, L.; Shaikh, M. M.; Ghosh, P. *Inorg. Chem.* **2008**, *47*, 230–240.
(16) Samantaray, M. K.; Pang, K.; Shaikh, M. M.; Ghosh, P. *Inorg. Chem.* **2008**, *47*, 4153–4165.
(17) Baba, E.; Cundari, T. R.; Firkin, I. *Inorg. Chim. Acta* **2005**, *358*, 2867–2875.
(18) Lee, M.-T.; Hu, C.-H. *Organometallics* **2004**, *23*, 976–983.
(19) Nemcsok, D.; Wichmann, K.; Frenking, G. *Organometallics* **2004**, *23*, 3640–3646.
(20) Vyboishchikov, S. F.; Frenking, G. *Chem.—Eur. J.* **1998**, *4*, 1439–1448.
(21) Frenking, G.; Pidun, U. *J. Chem. Soc., Dalton Trans.* **1997**, 1653–1662.
(22) Pernak, J.; Skrzypczak, A. *Eur. J. Med. Chem.* **1996**, *31*, 901–903.
(23) Andrews, J. M. *J. Antimicrob. Chemother.* **2001**, *48*, 5–16.
(24) Pernak, J.; Sobaszkiewicz, K.; Mirska, I. *Green Chem.* **2003**, *5*, 52–56.
(25) Cetinkaya, E.; Denizci, A.; Ozdemir, I.; Ozturk, H. T.; Karaboz, I.; Cetinkaya, B. *J. Chemother.* **2002**, *14*, 241–245.
(26) Demberelnyamba, D.; Kim, K.-S.; Choi, S.; Park, S.-Y.; Lee, H.; Kim, C.-J.; Yoo, I.-D. *Bioorg. Med. Chem.* **2004**, *12*, 853–857.
(27) Klasen, H. J. *Burns* **2000**, *26*, 117–130.
(28) Silver, S.; Phung, L.; Silver, G. *J. Ind. Microbiol. Biotechnol.* **2006**, *33*, 627–634.
(29) Moyer, C. A.; Brentano, L.; Gravens, D. L.; Margraf, H. W.; Monafo, W. W. *Arch. Surg.* **1965**, *90*, 812–867.
(30) Fox, C. L. *Arch. Surg.* **1968**, *96*, 184–188.
(31) Melaiye, A.; Youngs, W. *Expert Opin. Ther. Pat.* **2005**, *15*, 125–130.
(32) Klasen, H. J. *Burns* **2000**, *26*, 131–138.
(33) Fakhry, S. M.; Alexander, J.; Smith, D.; Meyer, A. A.; Petterson, H. D. *J. Burn Care Rehabil.* **1995**, *16*, 86–90.
(34) Russell, A. D.; Hugo, W. B. *Prog. Med. Chem.* **1994**, *31*, 351–370.
(35) Lansdown, A. B. *J. Wound Care* **2002**, *11*, 125–130.
(36) Feng, Q. L.; Wu, J.; Chen, G. Q.; Cui, F. Z.; Kim, T. N.; Kim, J. O. *J. Biomed. Mater. Res.* **2000**, *52*, 662–668.
(37) Modak, S. M.; Fox, C. L., Jr. *Biochem. Pharmacol.* **1973**, *22*, 2391–2404.
(38) Fox, C.; Modak, S. *Antimicrob. Agents Chemother.* **1974**, *5*, 582–588.
(39) Holt, K.; Bard, A. *Biochemistry* **2005**, *44*, 13214–13223.
(40) Bragg, P. D.; Rainnie, D. J. *Can. J. Microbiol.* **1974**, *20*, 883–889.
(41) Schreurs, W. J.; Rosenberg, H. *J. Bacteriol.* **1982**, *152*, 7–13.
(42) Lansdown, A. B. *J. Wound Care* **2002**, *11*, 173–177.
(43) Drake, P. L.; Hazelwood, K. *Ann. Occup. Hyg.* **2005**, *49*, 575–585.
(44) East, B. W.; Boddy, K.; Williams, E. D.; Macintyre, D.; Mclay, A. L. *Clin. Exp. Dermatol.* **1980**, *5*, 305–311.
(45) Lee, S. M.; Lee, S. H. *J. Dermatol.* **1994**, *21*, 50–53.
(46) Greene, R. M.; Su, W. P. *Am. Fam. Physician* **1987**, *36*, 151–154.
(47) Demling, R. H.; Disanti, L. *Wounds* **2001**, *13* (Suppl A), 5–15.
(48) Baldi, C.; Minoia, C.; Di Nucci, A.; Capodaglio, E.; Manzo, L. *Toxicol. Lett.* **1988**, *41*, 261–268.
(49) Hussain, S.; Anner, R. M.; Anner, B. M. *Biochem. Biophys. Res. Commun.* **1992**, *189*, 1444–1449.
(50) Fraser, J. F.; et al. *ANZ J. Surg.* **2004**, *74*, 139–142.
(51) Liu, J.; Kershaw, W. C.; Klaassen, C. D. *Toxicol. Appl. Pharmacol.* **1991**, *107*, 27–34.
(52) Baldi, C.; Minoia, A. C.; DiNucci, A.; Capodaglio, E.; Manzo, L. *Toxicol. Lett.* **1988**, *41*, 261–268.
(53) Hidalgo, E.; Dominguez, C. *Toxicol. Lett.* **1998**, *98*, 169–79.
(54) Owens, C. J.; Yarbrough, D. R.; Brackett, N. C. *Arch. Intern. Med.* **1974**, *134*, 332–335.
(55) Fullar, F. W.; Engler, P. E. *J. Burn Care Rehabil.* **1988**, *9*, 606–609.
(56) Jerrett, F.; Ellerbe, S.; Demling, R. *Am. J. Surg.* **1978**, *135*, 818–819.
(57) McHugh, S. L.; Moellering, R. C.; Hopkins, C. C.; Swartz, M. N. *Lancet* **1975**, *1*, 235–240.
(58) Gupta, A.; Silver, S. *Nat. Biotechnol.* **1998**, *16*, 888.
(59) Silver, S.; Lo, J-F.; Gupta, A. *APUA News* **1999**, *17*, 1–3.
(60) Gupta, A.; Matsui, K.; Lo, J-F.; Silver, S. *Nat. Med.* **1999**, *5*, 183–188.
(61) Silver, S. *FEMS Microbiol. Rev.* **2003**, *27*, 341–353.
(62) Garrison, J. C.; Youngs, W. J. *Chem. Rev.* **2005**, *105*, 3978–4008.
(63) Melaiye, A.; Simons, R. S.; Milsted, A.; Pingitore, F.; Wesdemiotis, C.; Tessier, C. A.; Youngs, W. J. *J. Med. Chem.* **2004**, *47*, 973–977.
(64) Melaiye, A.; Sun, Z.; Hindi, K.; Milsted, A.; Ely, D.; Reneker, D. H.; Tessier, C. A.; Youngs, W. J. *J. Am. Chem. Soc.* **2005**, *127*, 2285–2291.
(65) Reneker, D. H.; Yarin, A. L.; Fong, H.; Koombhongse, S. *J. Appl. Phys.* **2000**, *87*, 4531–4574.
(66) Kascatan-Nebioglu, A.; Melaiye, A.; Hindi, K.; Durmus, S.; Panzner, M.; Hogue, L.; Mallett, R.; Hovis, C.; Coughenour, M.; Crosby, S.; Milsted, A.; Ely, D.; Tessier, C.; Cannon, C.; Youngs, W. *J. Med. Chem.* **2006**, *49*, 6811–6818.
(67) Cropp, G. J. *Am. J. Med.* **1996**, *100* (1A), 19S–29S.
(68) Osman, F.; McCready, S. *Mol. Gen. Genet.* **1998**, *260*, 319–334.
(69) Abratt, V. R.; Peak, M. J.; Peak, J. G.; Santangelo, J. D.; Woods, D. R. *Can. J. Microbiol.* **1990**, *36*, 490–494.
(70) Selby, C. P.; Sancar, A. *Prog. Clin. Biol. Res.* **1990**, *340A*, 179–193.
(71) Hindi, K.; Siciliano, T.; Durmus, S.; Panzner, M.; Medvetz, D.; Reddy, V.; Hogue, L.; Hovis, C.; Hilliard, J.; Mallett, R.; Tessier, C.; Cannon, C.; Youngs, W. *J. Med. Chem.* **2008**, *51*, 1577–1583.
(72) Viciano, M.; Mas-Marza, E.; Sanau, M.; Peris, E. *Organometallics* **2006**, *25*, 3063–3069.

Downloaded by UNIV MAASTRICHT on August 28, 2009 | http://pubs.acs.org
Publication Date (Web): July 6, 2009 | doi: 10.1021/cr800500u

(73) Ray, S.; Mohan, R.; Singh, J. K.; Samantaray, M. K.; Shaikh, M. M.; Panda, D.; Ghosh, P. *J. Am. Chem. Soc.* **2007**, *129*, 15042–15053.
(74) Medvetz, D. A.; Hindi, K. M.; Panzner, M. J.; Ditto, A. J.; Yun, Y. H.; Youngs, W. J. *Met.-Based Drugs* **2008**, *2008*, 384010.
(75) Barnard, P.; Wedlock, L.; Baker, M.; Berners-Price, S.; Joyce, D.; Skelton, B.; Steer, J. *Angew. Chem., Int. Ed.* **2006**, *45*, 5966–5970.
(76) Barnard, P.; Baker, M.; Berners-Price, S.; Day, D. *J. Inorg. Biochem.* **2004**, *98*, 1642–1647.
(77) Berners-Price, S. J.; Johnson, R. K.; Giovenella, A. J.; Faucette, L. F.; Mirabelli, C. K.; Sadler, P. J. *J. Inorg. Biochem.* **1988**, *33*, 285–295.
(78) Thati, B.; Noble, A.; Creaven, B.; Walsh, M.; McCann, M.; Kavanagh, K.; Devereux, M.; Egan, D. *Cancer Lett.* **2007**, *248*, 321–331.
(79) Zhu, H.; Zhang, X.; Liu, X.; Wang, X.; Liu, G.; Usman, A.; Fun, H. *Inorg. Chem. Commun.* **2003**, *6*, 1113–1116.
(80) Liu, J.; Galettis, P.; Farr, A.; Maharaj, L.; Samarasinha, H.; McGechan, A.; Baguley, B.; Bowen, R.; Berners-Price, S.; McKeage, M. *J. Inorg. Biochem.* **2008**, *102*, 303–310.
(81) Elsome, A. M.; Hamilton-Miller, J. M. T.; Brumfitt, W.; Noble, W. C. *J. Antimicrob. Chemother.* **1996**, *37*, 911–918.
(82) Berners-Price, S. J.; Mirabelli, C. K.; Johnson, R. K.; Mattern, M. R.; McCabe, F. L.; Faucette, L. F.; Sung, C-M.; Mong, S-M.; Sadler, P. J.; Crooke, S. T. *Cancer Res.* **1986**, *46*, 5486–5493.
(83) Hoke, G. D.; Macia, R. A.; Meunier, P. C.; Bugelski, P. J.; Mirabelli, C. K.; Rush, G. F.; Matthews, W. D. *Toxicol. Appl. Pharmacol.* **1989**, *100*, 293–306.
(84) McKeage, M. J.; Berners-Price, S. J.; Galettis, P.; Bowen, R. J.; Brouwer, W.; Ding, L.; Zhuang, L.; Baguley, B. C. *Cancer Chemother. Pharmacol.* **2000**, *46*, 343–350.
(85) Fricker, S. P. *Gold Bull.* **1996**, *29*, 53–60.
(86) Merchant, B. *Biologicals* **1998**, *26*, 49–59.
(87) Shaw, C. F., III *Chem. Rev.* **1999**, *99*, 2589–2600.
(88) Simon, T. M.; Kunishima, D. H.; Vibert, G. J.; Lorber, A. *Cancer Res.* **1981**, *41*, 94–97.
(89) Mirabelli, C. K.; Johnson, R. K.; Sung, C. M.; Faucette, L. F.; Muirhead, K.; Crooke, S. T. *Cancer Res.* **1985**, *45*, 32–39.
(90) McKeage, M. J.; Maharaj, L.; Berners-Price, S. J. *Coord. Chem. Rev.* **2002**, *232*, 127–135.
(91) McKeage, M. J. *Br. J. Pharmacol. Rev.* **2002**, *136*, 1081–1082.
(92) Rigobello, M. P.; Scutari, G.; Folda, A.; Bindoli, A. *Biochem. Pharmacol.* **2004**, *67*, 689–696.
(93) Barnard, P. J.; Berners-Price, S. J. *Coord. Chem. Rev.* **2007**, *251*, 1889–1902.
(94) Urig, S.; Fritz-Wolf, K.; Reau, R.; Herold-Mende, C.; Toth, K.; Davioud-Charvet, E.; Becker, K. *Angew. Chem., Int. Ed.* **2006**, *45*, 1881–1886.
(95) Cronje, S.; Raubenheimer, H. G. *Chem. Soc. Rev.* **2008**, *37*, 1998–2011.
(96) Elsome, A. M.; Hamilton-Miller, J. M. T.; Brumfitt, W.; Nobble, W. C. *J. Antimicrob. Chemother.* **1996**, *37*, 911–918.
(97) Nomiya, K.; Noguchi, R.; Ohsawa, K.; Tsuda, K.; Oda, M. *J. Inorg. Biochem.* **2000**, *78*, 363–370.
(98) Özdemir, I.; Denizci, A.; Öztürk, T. H.; Çetinkaya, B. *Appl. Organometal. Chem.* **2004**, *18*, 318–322.
(99) Baker, M. V.; Barnard, P. J.; Berners-Price, S. J.; Brayshaw, S. K.; Hickey, J. L.; Skelton, B. W.; White, A. H. *Dalton Trans.* **2006**, 3708–3715. http://dx.doi.org/10.1039/b602560a.
(100) Barnard, P. J.; Baker, M. V.; Berners-Price, S. J.; Skelton, B. W.; White, A. H. *Dalton Trans.* **2004**, 1038–1047.
(101) Baker, M. V.; Barnard, P. J.; Berners-Price, S. J.; Brayshaw, S. K.; Hickey, J. L.; Skelton, B. W.; White, A. H. *J. Organomet. Chem.* **2005**, *690*, 5625–5635.
(102) Horvath, U. E. I.; Bentivoglio, G.; Hummel, M.; Schottenberger, H.; Wurst, K.; Nell, M. J.; van Rensburg, C. E. J.; Cronje, S.; Raubenheimer, H. G. *New J. Chem.* **2008**, *32*, 533–539.
(103) Jellicoe, M. M.; Nichols, S. J.; Callus, B. A.; Baker, M. V.; Barnard, P. J.; Berners-Price, S. J.; Whelan, J.; Yeoh, G. C.; Filipovska, A. *Carcinogenesis* **2008**, *29*, 1124–1133.
(104) Hickey, J. L.; Ruhayel, R. A.; Barnard, P. J.; Baker, M. V.; Berners-Price, S. J.; Filipovska, A. *J. Am. Chem. Soc.* **2008**, *130*, 12570–12571.
(105) Alessio, E.; Mestroni, G.; Bergamo, A.; Sava, G. *Curr. Top. Med. Chem.* **2004**, *4*, 1525–1535.
(106) Clarke, M.; Zhu, F.; Frasca, D. *Chem. Rev.* **1999**, *99*, 2511–2534.
(107) Keppler, B. K.; Rupp, W. *J. Cancer Res. Clin. Oncol.* **1986**, *111*, 166–168.
(108) Yasbin, R. E.; Matthews, C. R.; Clarke, M. J. *Chem.-Biol. Interactions* **1980**, *31*, 355–365.
(109) Morris, R. E.; Aird, R. E.; Murdoch, P. S.; Chen, H.; Cummings, J.; Hughes, N. D.; Parsons, S.; Parkin, A.; Boyd, G.; Jodrell, D. I.; Sadler, P. J. *J. Med. Chem.* **2001**, *44*, 3616–3621.
(110) Hotze, A. C. G.; Bacac, M.; Velders, A. H.; Jansen, B. A. J.; Kooijman, H.; Spek, A. L.; Haasnoot, J. G.; Reedijk, J. *J. Med. Chem.* **2003**, *46*, 1743–1750.
(111) Vliet, P. M.; Toekimin, S. M. S.; Haasnoot, J. G.; Reedijk, J.; Novakova, O.; Vrana, O.; Brabec, V. *Inorg. Chim. Acta* **1995**, *231*, 57–64.
(112) Chifotides, H. T.; Dunbar, K. R. *Acc. Chem. Res.* **2005**, *38*, 146–156.
(113) Mestroni, G.; Alessio, E.; Santi, A. S.; Geremia, S.; Bergamo, A.; Sava, G.; Boccarelli, A.; Schettino, A.; Coluccia, M. *Inorg. Chim. Acta* **1998**, *273*, 62–71.
(114) Qu, P.; He, H.; Liu, X. *Huaxue Jinzhan* **2006**, *18*, 1646–1651.
(115) Bruijnincx, P. C. A.; Sadler, P. J. *Curr. Opin. Chem. Biol.* **2008**, *12*, 197–206.
(116) Reedijk, J. *Platinum Met. Rev.* **2008**, *52*, 2–11.
(117) Tselepi-Kalouli, E.; Katsaros, N.; Sideris, E. *Inorg. Chem. Acta* **1986**, *124*, 181–186.
(118) Kapitza, S.; Pongratz, M.; Jakupec, M. A.; Heffeter, P.; Berger, W.; Lackinger, L.; Keppler, B. K.; Marian, B. *J. Cancer Res. Clin. Oncol.* **2005**, *131*, 101–110.
(119) Frasca, D.; Ciampa, J.; Emerson, J.; Umans, R. S.; Clarke, M. J. *Met.-Based Drugs* **1996**, *3*, 197–209.
(120) Cetinkaya, B.; Özemir, I.; Binbasioglu, B.; Durmaz, R.; Gunal, S. *Arzneim.-Forsch./Drug Res.* **1999**, *49*, 538–540.
(121) Cetinkaya, B.; Cetinkaya, E.; Kucukbay, H.; Durmaz, R. *Arzneim.-Forsch./Drug Res.* **1996**, *46*, 821–823.
(122) Navarro, M.; Penã, N. P.; Colmenares, I.; González, T.; Arsenak, M.; Taylor, P. *J. Inorg. Biochem.* **2006**, *100*, 152–157.
(123) Friebolin, W.; Schilling, G.; Zoller, M.; Amtmann, E. *J. Med. Chem.* **2005**, *48*, 7925–7931.
(124) Gonzalez, M. L.; Tercero, J. M.; Matilla, A.; Niclos-Gutierrez, J.; Fernandez, M. T.; Lopez, M. C.; Alonso, C.; Gonzalez, S. *Inorg. Chem.* **1997**, *36*, 1806–1812.
(125) Budzisz, E.; Krajewska, U.; Rozalski, M.; Szulawska, A.; Czyz, M.; Nawrot, B. *Eur. J. Pharmacol.* **2004**, *502*, 59–65.
(126) Kovala-Demertzi, D.; Demertzis, M. A.; Filiou, E.; Pantazaki, A. A.; Yadav, P. N.; Miller, J. R.; Zheng, Y.; Kyriakidis, D. A. *BioMetals* **2003**, *16*, 411–418.
(127) Kuduk-Jaworska, J.; Puszko, A.; Kubiak, M.; Pełczynska, M. *J. Inorg. Biochem.* **2004**, *98*, 1447–1456.
(128) Zhao, G.; Lin, H.; Yu, P.; Sun, H.; Zhu, S.; Su, X.; Chen, Y. *J. Inorg. Biochem.* **1999**, *73*, 145–149.
(129) Kovala-Demertzi, D.; Boccarelli, A.; Demertzis, M. A.; Coluccia, M. *Chemotherapy* **2007**, *53*, 148–152.
(130) Friaza, G. G.; Fernández-Botello, A.; Pérez, J. M.; Prieto, M. J.; Moreno, V. *J. Inorg. Biochem.* **2006**, *100*, 1368–1377.
(131) Ruiz, J.; Cutillas, N.; Vicente, C.; Villa, M. D.; López, G. *Inorg. Chem.* **2005**, *44*, 7365–7376.
(132) Abu-Surrah, A. S.; Al-Allaf, T. A. K.; Rashan, L. J.; Klinga, M.; Leskelä, M. *Eur. J. Med. Chem.* **2002**, *37*, 919–922.
(133) Faraglia, G.; Fregona, D.; Sitranb, S.; Giovagninia, l.; Marzanoc, C.; Baccichetti, F.; Casellato, U.; Graziani, R. *J. Inorg. Biochem.* **2001**, *83*, 31–40.
(134) Suvachittanont, S.; Hohmann, H.; van Eldik, R.; Reedijk, J. *Inorg. Chem.* **1993**, *32*, 4544–4548.
(135) Abu-Surrah, A. S.; Al-Sa'doni, H. H.; Abdalla, M. Y. *Cancer Ther.* **2008**, *6*, 1–10.
(136) Caires, A. C. F. *Anti Canc. Agents Med. Chem.* **2007**, *7*, 484–491.
(137) Hermann, W. A.; Bohn, V. P. W.; Gstottmayr, C. W. K.; Grosche, M.; Reisinger, C.-P.; Weskamp, T. *J. Organomet. Chem.* **2001**, *617–618*, 616–628.
(138) Gupta, K.; Bishop, J.; Peck, A.; Brown, J.; Wilson, L.; Panda, D. *Biochemistry* **2004**, *43*, 6645–6655.
(139) Mueller, S.; Schittenhelm, M.; Honecker, F.; Malenke, E.; Lauber, K; Wesselborg, S.; Hartmann, J. T.; Bokemeyer, C.; Mayer, F. *Int. J. Oncol.* **2006**, *29*, 471–479.
(140) Billecke, C.; Finniss, S.; Tahash, L.; Miller, C.; Mikkelsen, T.; Farell, N. P.; Bogler, O. *Neuro Oncol.* **2006**, *8*, 215–226.
(141) Hagting, A.; Karlsson, C.; Clute, P.; Jackman, M.; Pines, J. *EMBO J.* **1998**, *17*, 4127–4138.

CR800500U

Downloaded by UNIV MAASTRICHT on August 28, 2009 | http://pubs.acs.org
Publication Date (Web): July 6, 2009 | doi: 10.1021/cr800500u